Title
A 1.2-1.9 BeV/c, SEPARATED K~ MESON BEAM: DESIGN AND CONSTRUCTION

Authors
Button-Shafer, Janice
Kalbfleisch, George R.
Miller, Donald H.
et al.

Publication Date
1966-07-28

UCRL-17018

University of California

Ernest O. Lawrence Radiation Laboratory

A 1.2-1.9 BeV/c, SEPARATED K^- MESON BEAM: DESIGN AND CONSTRUCTION

DISCLAIMER

UCRL-17018
UC-37 Instruments
TID-4500 (48th Ed.)

UNIVERSITY OF CALIFORNIA

Lawrence Radiation Laboratory
Berkeley, California

AEC Contract No. W-7405-eng-48

A 1.2 - 1.9 BeV/c, SEPARATED K^- MESON BEAM: DESIGN AND CONSTRUCTION

Janice Button-Shafer, George R. Kalbfleisch, Donald H. Miller, Janos Kirz, Charles G. Wohl, J. Richard Hubbard, Darrell O. Huwe, Harold K. Ticho and Donald H. Stork

July 28, 1966

Printed in USA. Price $3.00. Available from the Clearinghouse for Federal Scientific and Technical Information, National Bureau of Standards, U. S. Department of Commerce, Springfield, Virginia.

A 1.2-1.9 BeV/c, SEPARATED K^- MESON BEAM: DESIGN AND CONSTRUCTION

Contents

A 1.2-1.9 BeV/c, SEPARATED K^- MESON BEAM: DESIGN AND CONSTRUCTION

Janice Button-Shafer, George R. Kalbfleisch, Donald H. Miller, Janos Kirz, Charles G. Wohl, J. Richard Hubbard, and Darrell O. Huwe

Lawrence Radiation Laboratory
University of California, Berkeley, California

and

Harold K. Ticho and Donald H. Stork

University of California at Los Angeles
Los Angeles, California

July 28, 1966

ABSTRACT

Because of repeated inquiries concerning the design of the "K-72" separated beam, a rough description of some of the design considerations and tuning results is presented here.*

This report describes the design and operation of a variable-momentum, separated K^- meson beam for an experiment in the 72-inch hydrogen bubble chamber at the Bevatron. The beam momentum was variable over the region 1.25 to 1.95 BeV/c. With two stages of electromagnetic separation, the beam channel measured 155 ft (target to bubble chamber); it afforded a pion rejection factor of about 10^5. The K^- meson flux at the chamber was about 10 K^- per 10^{11} protons at the higher momenta, and somewhat less at the lower. Beam contamination (by pions and muons) was $\leq$ 10 percent. A total exposure of about 14,000 events per millibarn was made.

---

*Although UCLA physicists Ticho and Stork did most of the primary design work, they bear little or no responsibility for statements here. The writers intended this paper as a first draft and apologize for unevenness in emphasis.

I. INTRODUCTION

For the purpose of studying the Ξ hyperon and various resonant states of the K^*, Y^*, and Ξ^* variety, an extended exposure of the LRL 72-inch hydrogen bubble chamber to a separated beam of negative K mesons was made between September 1961 and June 1962. This paper describes the design, construction, and operation of the beam (called the "K-72 beam") for that experiment. The requirements of the beam were several: (1) a variable momentum; (2) a separation of K^-'s from other components; (3) a reasonable K flux (7 to 10 K's per pulse) at the bubble chamber. An earlier separated K^- beam at 1.15 BeV/c is described in Ref. 1, to which the reader is referred for a more extensive discussion of some of the design techniques for such beams.

A. Variable-Momentum Requirement

The threshold for interactions such as $K^-p \rightarrow \Xi K$ or $K^-p \rightarrow N\overline{K}^*$ is 1.05 BeV/c. Flexibility of beam optics was required in order to study the various interactions as functions of beam momentum. The K-72 beam was designed to operate between 1.25 and 1.95 BeV/c. Particles entering the beam channel were produced in a target flipped into the narrow circulating proton beam late in the acceleration cycle of the Bevatron. Negative secondary particles were bent outward into a hole through the yoke of the Bevatron magnet. The beam optics was adjusted to accept only those particles produced at 0° with respect to the proton beam; thus the horizontal image width was determined by the radial dimension of the target. With this angle fixed, the momentum of the particles entering the exit channel from the Bevatron tank was determined mainly by the position of the target relative to it (for a given magnetic field). Thus a movable target was necessary in order to achieve the variable momentum. Two targets situated at different radii from the center of the Bevatron quadrant, both of which could be moved azimuthally, were used. A magnet in the exit channel in the Bevatron magnet yoke provided corrective steering for outgoing particles of extreme momenta. The currents in the magnets in the beam-transport system were scaled to provide the proper fields for the different momenta. However some extra trimming of fields was required, as will be discussed below.

B. Separation of K's

The second requirement was the separation of the K's from the much more numerous π's and μ's. The number of π's accepted by the beam channel was more than 10^5 per pulse (with K's about 10^3 per pulse). Many μ's resulted from the decay of π's and K's. Some separation scheme which would give a rejection factor of about 10^5 was needed to prevent the bubble chamber from being flooded by π and μ tracks. [Any appreciable contamination would produce events with topologies identical to those of interesting K^- interactions (e.g., $\pi^-p \rightarrow \Lambda K^0$ might be interpreted as $K^-p \rightarrow \Xi^0 K^0$).]

Crossed electric- and magnetic-field spectrometers were used to achieve the separation after momentum analysis by the Bevatron magnetic field. The spectrometers, which permitted separation on the basis of particle

velocity, were arranged to deflect π's and μ's out of the horizontal plane, but to pass K's undeflected; they served as filters which passed only particles of the proper mass.

The optical arrangement for the velocity selection is shown in Fig. 1. The spectrometer, providing a horizontal magnetic field (H) and a vertical electric field (E), will not deflect particles with

$$\beta_0 = \frac{|E|}{|H|} ,$$

β being the velocity in units of c. This is seen immediately from the force equation

$$\vec{F} = e(\vec{E} + \vec{\beta}\times\vec{H}).$$

Particles with velocity β different from β_0 and with energy W will suffer an angular deflection of

$$\Delta\theta = \frac{VL}{d} \cdot \frac{1}{p}\left(\frac{1}{\beta_0} - \frac{1}{\beta}\right) = \frac{VL}{d} \cdot \frac{(W_0 - W)}{p^2}$$

where p = momentum in MeV/c, W = total energy in MeV, V = voltage between spectrometer plates in millions of volts, d = separation of plates, and L = effective length of plates. The desired suppression of π's and μ's relative to K's is then achieved by placing a slit at a vertical focus after the spectrometer. For a given geometry and voltage the parameter of interest is $(W_K - W_\pi)/p^2$. This is shown as a function of momentum in Fig. 2. Since the value of β for a particle is determined by the ratio p/m, it is evident that for a π or a μ to traverse the system undeflected it would have to have a much lower momentum than a K; and thus it would be eliminated by the momentum-selecting elements of the system.

The pion-rejection factor (η) at the slit is determined by the ratio of π and K image separation S to image size W. For the optical arrangement of Fig. 1, this is given by:

$$\eta = \frac{S}{W} = \frac{P}{T} \cdot \Delta\theta$$

where P is the object distance and T is the vertical dimension of the target. Ideally, η should be much greater than 1.

In order for the desired suppression of π's and μ's to be obtained, η had to be about two in each of the separation stages. For an ideal system a perfect separation could be achieved by decreasing T. (Increasing P leads to a loss of flux for a given plate separation d). However, the images were necessarily enlarged by several effects: (a) target "halo" effect and collimator scattering; (b) multiple scattering of the beam in gases and windows in the beam channel; (c) chromatic and spherical aberrations of the focusing elements of the system. There was little point in making the actual target height much

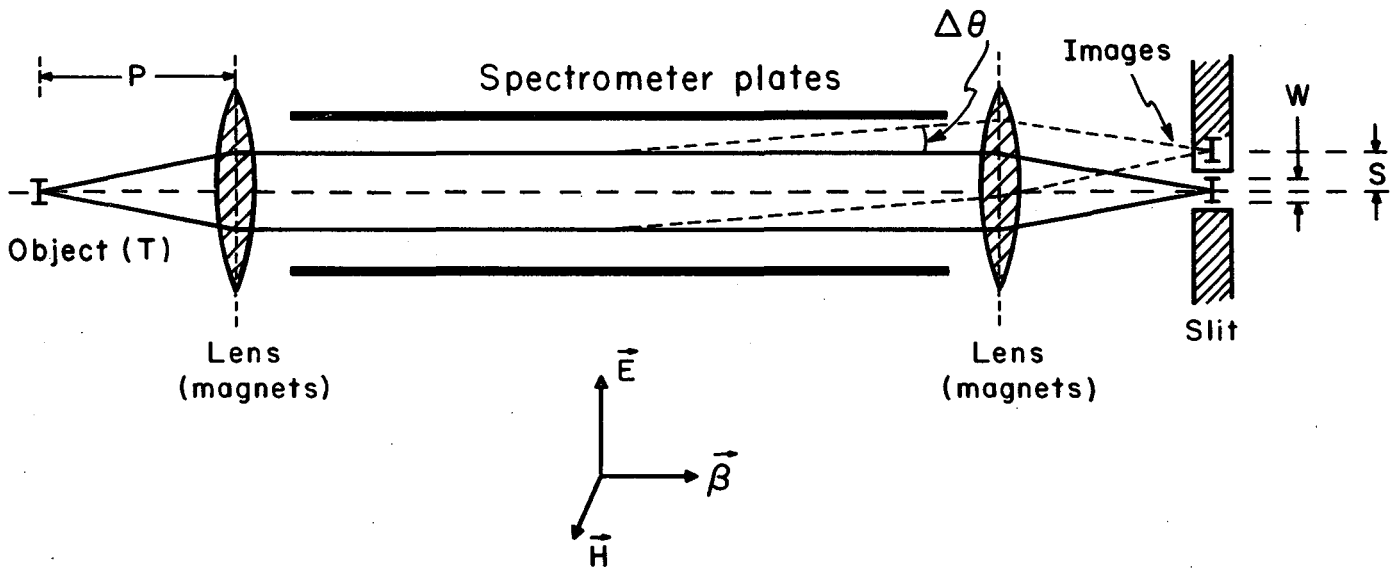

MUB-12817

Fig. 1. The optical scheme for a crossed electric- and magnetic-field spectrometer. The spectrometer and slit act as a filter which transmits particles with $\beta_0 = E/H$. With momentum selection before and after the spectrometer, the device thus becomes a mass spectrometer.

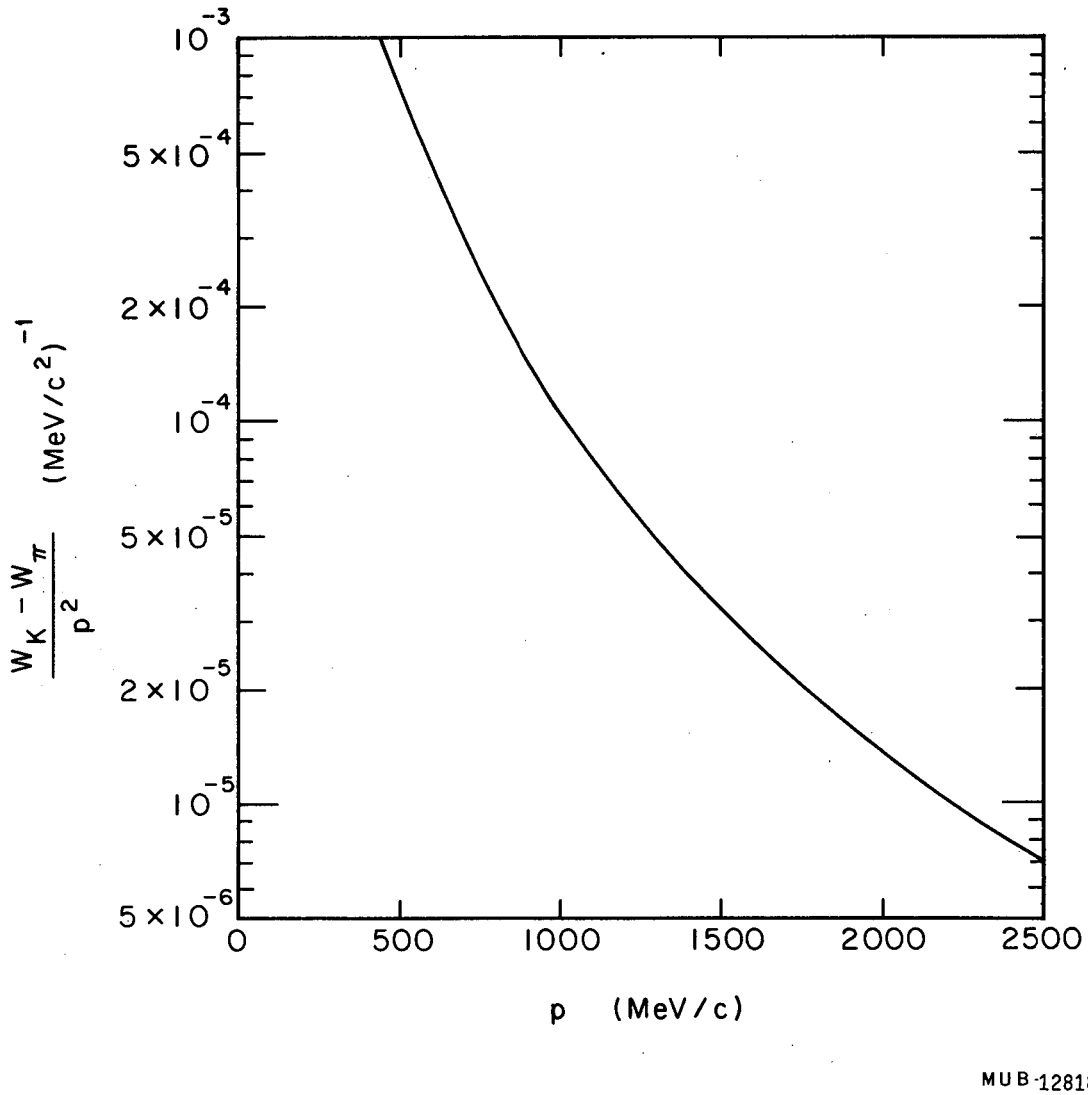

Fig. 2. For a fixed geometry and voltage of the spectrometer system, the angle of deflection $\Delta\theta$ for pions relative to K mesons is proportional to $(W_K - W_\pi)/p^2$.

smaller than the apparent size it would have because of these effects alone.

The first effect was greatly reduced by collimating the beam at a number of points along its length in both the horizontal and vertical planes, and by using two stages of separation. The slit at the end of the first stage acted as the source for the second stage. Looking "upstream" from the first slit, the system "saw" not only the target but also a surrounding "halo" due to decays of other particles. This halo did not exist for the second stage, since all that the system saw was the slit. This cleaner source for the second stage (as well as some intermediate momentum analysis) made the two-stage separation scheme much more effective than a single stage of twice the spectrometer length would have been.

For minimization of multiple scattering of beam particles, the beam line was coupled to the Bevatron vacuum tank. Except for very thin Mylar windows which isolated the spectrometers, the beam pipe was evacuated from the Bevatron to a point just in front of the first slit, and from the rear of this slit to the entrance of the second slit. The windows at the ends of the vacuum sections were also of thin Mylar. These windows and the short lengths of unevacuated beam path caused negligible broadening of the target and slit images.

The extensive measures taken to correct chromatic and spherical aberrations are discussed in detail below.

C. Beam Flux

For optimum use of the bubble chamber, an incident flux of ≤ 10 K^- per pulse was desired. It is this upper limit on the number of particles per pulse which makes practical the use of a long beam line with extensive separation stages. The beam path length was 155 feet. Only about 1% of the K mesons survived for the median beam momentum. In order to obtain the 10 K^- per pulse with the average Bevatron intensity of 10^{11} protons per pulse, it is necessary to use a "momentum bite" of nearly 6% full width. This introduced another problem: chromatic aberrations would have doubled the width of the images and thus made separation of π's and K's impossible with the limited values of η which could be obtained. To correct such aberrations, bending-magnet shims were employed to make both separation stages give achromatic images at the slits. This was a major effort and will be described in detail below. It was also found possible to reduce the nonlinear aberrations of the quadrupoles with shims, and thus further increase the quality of the images. All magnets in the system were extensively studied by wire-orbit work.

II. BEAM LAYOUT AND OPTICS

The layout of the beam is displayed in Fig. 3. Particles produced in the target and passing out of the Bevatron vacuum chamber through the exit channel were steered by M1 and then entered the first of two separation stages. This consisted of the quadrupole doublet Q1, the spectrometer S1, bending magnets M2 and M3, and the first slit, located inside the singlet quadrupole Q2. The slit acted as the source for the second stage, which consisted of bending magnets M4 and M5, the spectrometer S2, the quadrupole

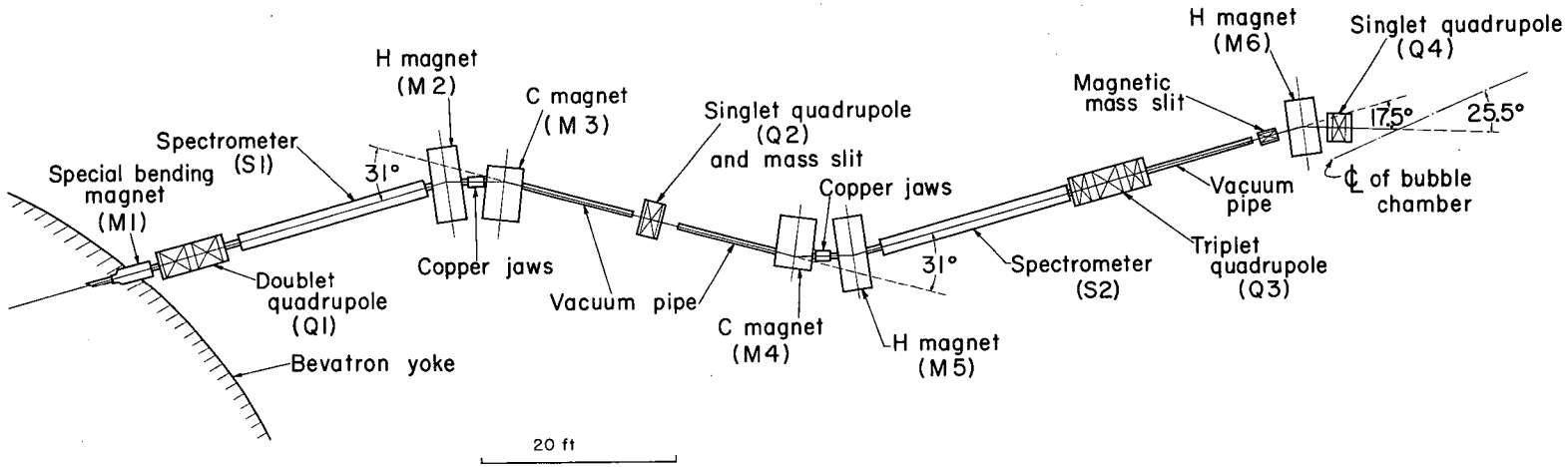

Fig. 3. Schematic of the beam channel. Particles produced in the target (not shown) pass through the Bevatron yoke and are steered by M1 to enter the first separation stage with the proper direction. The first stage extends to the first slit, located in Q2. The second stage is essentially a reflection of the first. M6 sweeps out any remnant of off-momentum components.

triplet Q3, and the second slit. After this was a bending magnet M6, a quadrupole singlet Q4, and finally the bubble chamber. There were adjustable-width jaws between each of the bending magnet pairs M2-M3 and M4-M5. Photographs of sections of the beam line are shown in Figs. 4 through 6. The ray diagrams of Fig. 7 show the optical effects of each of the beam elements.

A. Horizontal-Plane Optics

In the horizontal plane, Q1 focused the target onto the M2-M3 pair. The momentum dispersion ($\Delta\lambda/\Delta p$) caused by the Bevatron magnetic field resulted in a spatial distribution of the foci of the momentum components along a somewhat skew line centered at the jaws in M2-M3. The adjustable jaws then selected the momentum bite, which during operation was 3% on either side of the central momentum. The horizontal image size at the jaws for a given momentum was about 0.6 inch, and the dispersion of images was about 0.5 inch per 1% dp/p. The bend of 31° caused by M2 and M3 provided the necessary vertical focusing (see below); also, as its dispersion approximately cancelled the dispersion caused by the Bevatron, the magnet pair kept the horizontal width of the beam small so that it passed through Q2 without loss of flux at the sides. The quadrupole Q2 focused the first pair of jaws onto the second, located in M4-M5. This carried the horizontal dispersion of the momentum components from M2-M3 to M4-M5. The pair M4-M5 bent the beam back through 31° (again as required by the vertical optics) and steered the beam to the quadrupole triplet Q3; it also reduced the dispersion so that all the beam would pass through Q3. Quadrupole Q3 focused the second jaws onto the center of the bubble chamber. The bending magnet M6 steered the beam into the chamber, sweeping out any remnant of off-momentum components (consisting mostly of muons from pion decay).

The different momentum components would have been spatially distributed equally in the chamber if the M6 bend had been reversed. This condition would have been desirable but was prevented by construction work preparatory to a Bevatron modification program. Thus the beam was rather tightly packed upon entering the chamber. As a partial remedy for this, quadrupole Q4 was available to help spread the beam in the horizontal plane.

Collimation in the horizontal plane cut out unwanted scattered and decay particles, as well as defined the momentum interval of the beam. Thus in addition to the jaws at the bends, there were collimators in the Bevatron exit channel and in Q1, Q2, Q3, and M6. The collimator in M6 closely matched the actual beam size both horizontally and vertically for as much reduction of contamination as possible.

B. Vertical-Plane Optics

In the vertical plane, quadrupole Q1 focused particles coming from the target in such a way that the central momentum rays were made parallel. High-momentum components diverged slightly inside the spectrometer. When set for K^- transmission, the spectrometers deflected the lighter pions and muons upwards. To prevent scattering of these diverging and deflected particles from the spectrometer plates back into the beam, the plates of S1 had a non-uniform separation, which was widest at the downstream end.

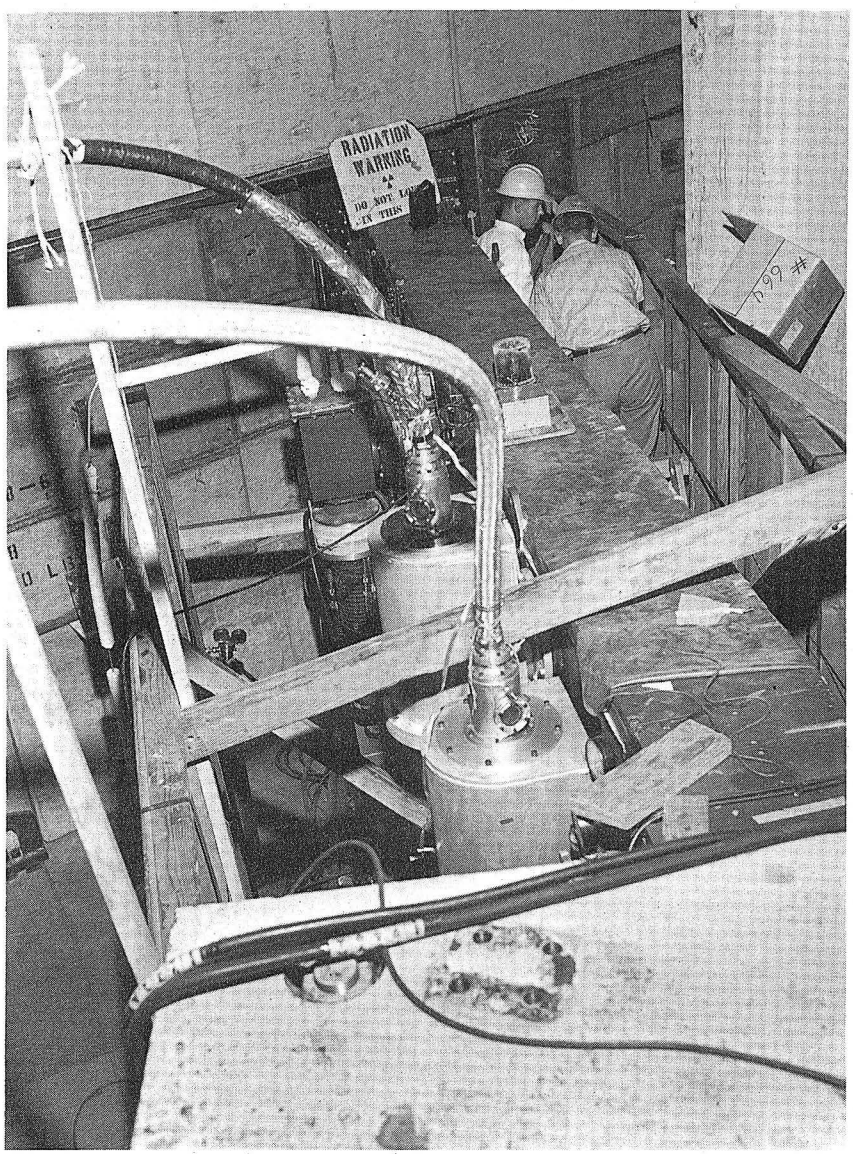

ZN-5708

Fig. 4. Photograph of part of the first stage, showing Bevatron shielding, the 20-foot spectrometer S1, and a corner of the H-magnet M2 as viewed from the first bend.

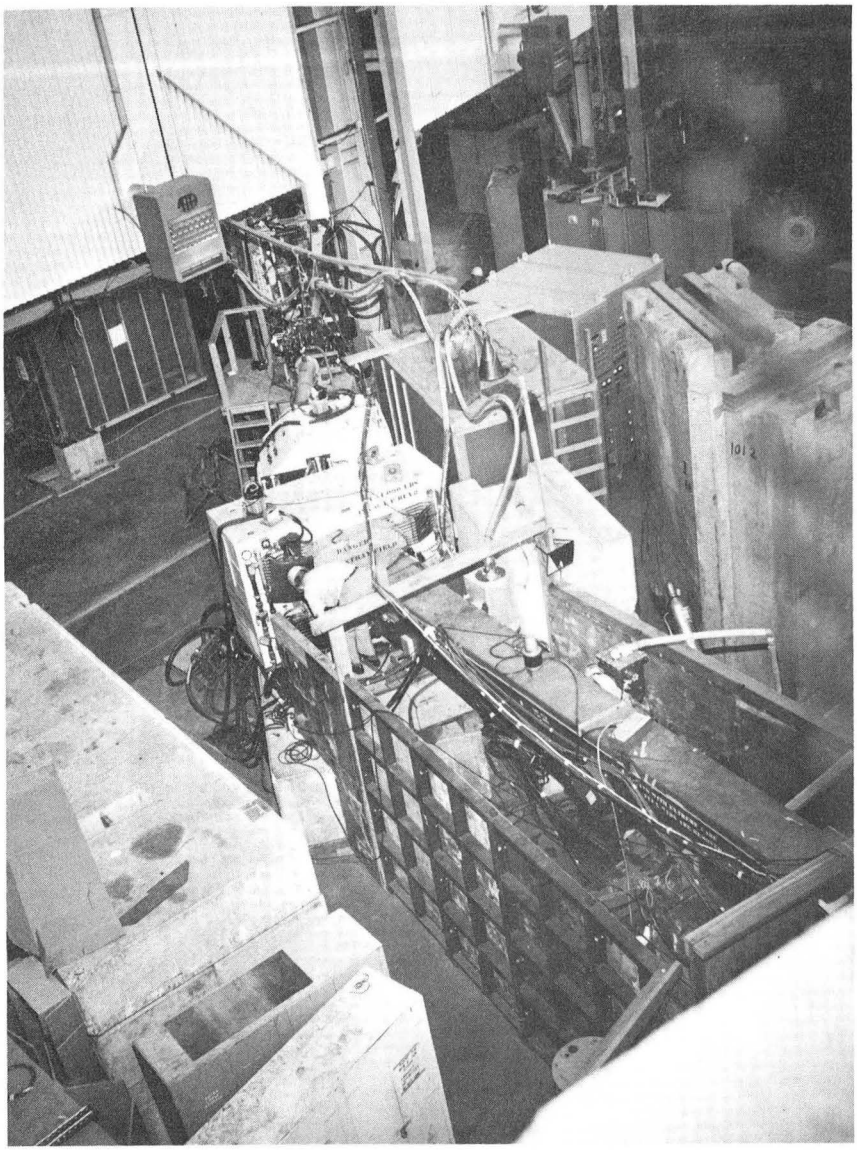

ZN-5707

Fig. 5. Photograph of part of the second stage, including Q2 (mass slit 1), C and H magnets M3 and M4 (bend 2), and spectrometer S2, in foreground. The connections for pole-face windings are barely visible on the downstream side of the C magnet (in the middle of the bend).

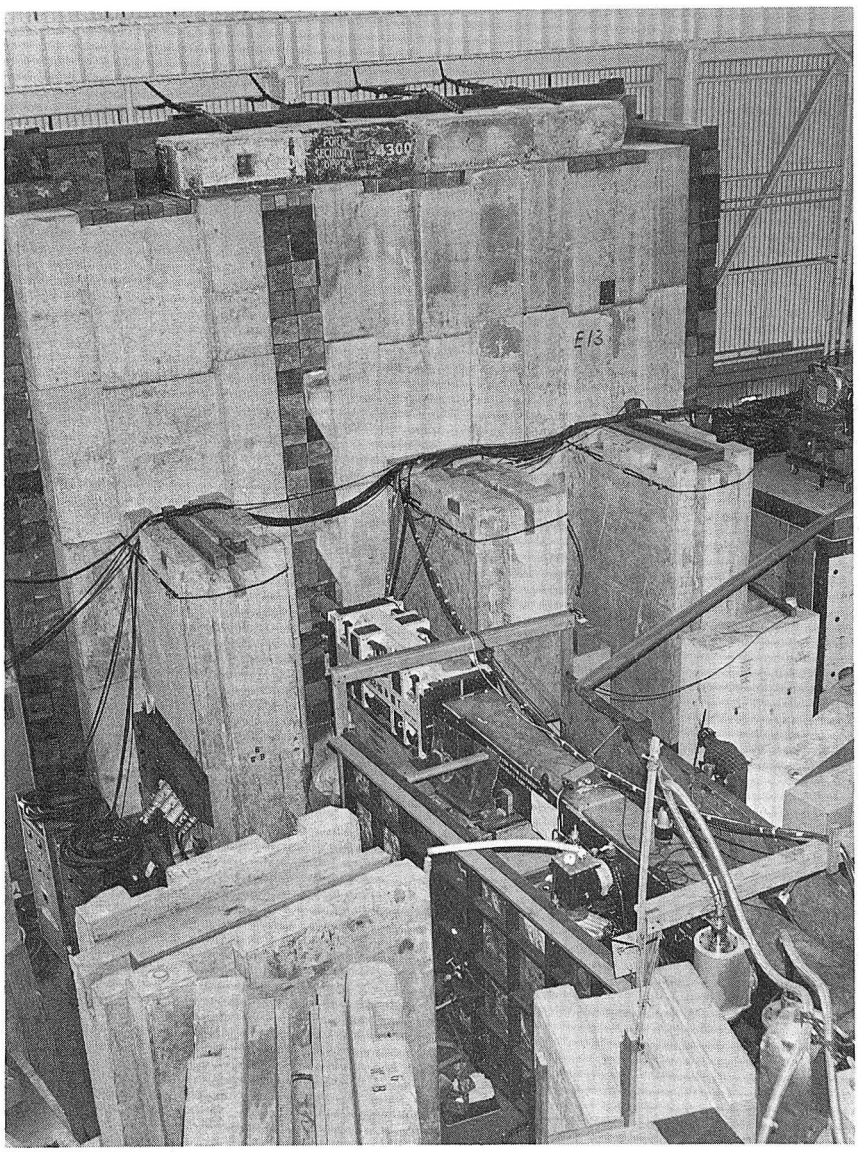

ZN-5706

Fig. 6. Downstream view of S2 and Q3 in second stage. The concrete shielding prevents stray flux (mostly composed of neutrons) from causing an appreciable background of events in the bubble chamber.

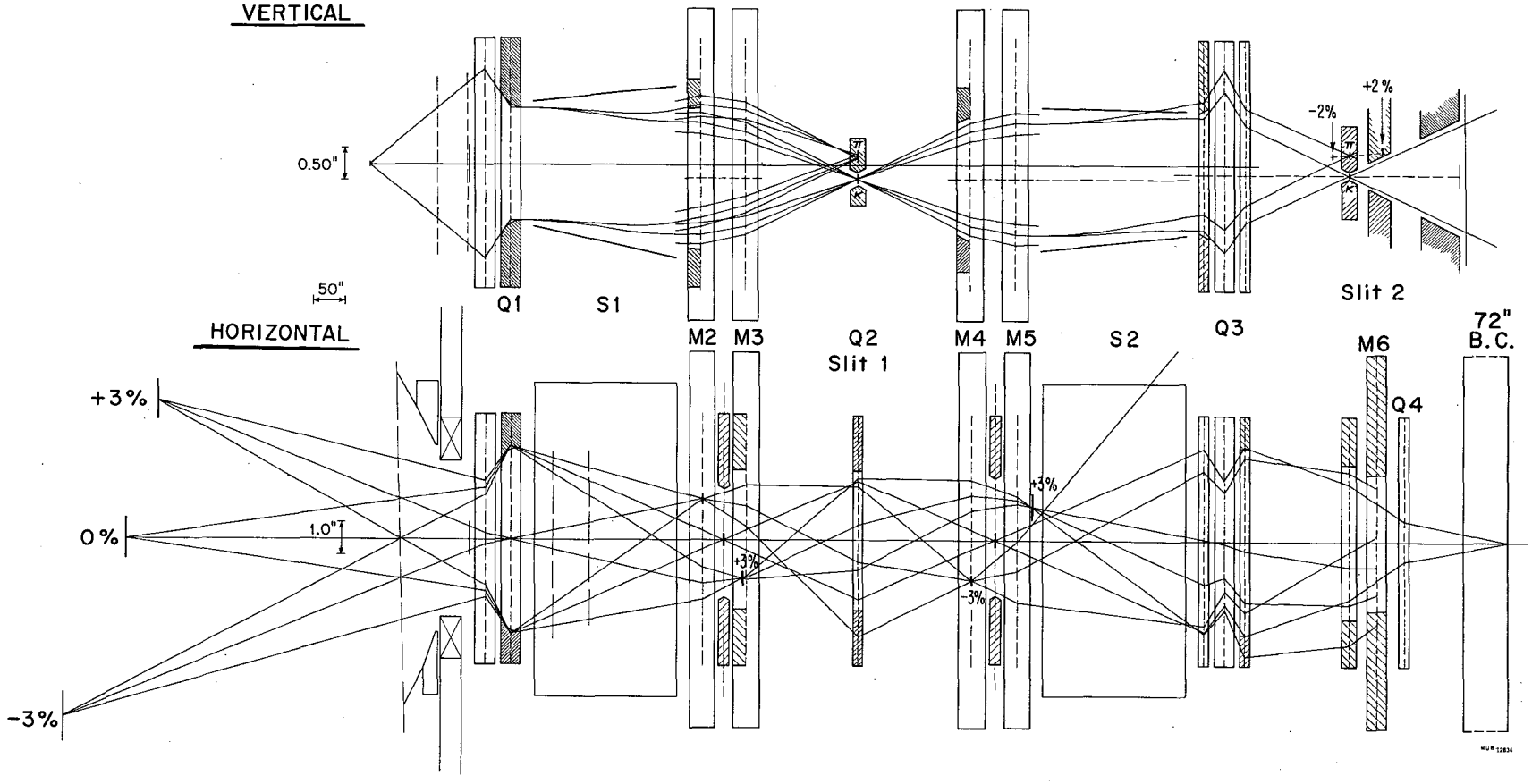

Fig. 7. Schematic of the horizontal and vertical optics at 1.55 BeV/c. Rays are drawn for the central momentum and for ± 3% dp/p. Collimation is indicated by cross hatching.

This arrangement caused the trajectories to drop about 0.2 inch, since at the upstream end the electrical force predominated, whereas at the downstream end the magnetic force was the stronger.

The effect in the vertical plane of the bending magnets M2 and M3 was to focus the beam at slit 1. This focus had to be achromatic in order to keep the image widths as small as possible. This was the reason for the dispersed horizontal focusing of the momentum components at this pair of magnets: they were carefully shimmed so that the magnetic field varied properly as a function of horizontal position across the beam to provide the correct vertical focal length for the momentum at each point, thus correcting the chromatic aberrations of the Bevatron field and of Q1. (The shimming is described below, and in the Appendix.) The vertical aperture of slit 1 varied from 0.120 inch at low momenta to 0.090 inch at high momenta.

Similarly the bending magnets M4 and M5 were shimmed to balance the chromatic aberrations of Q3 and thus to provide an achromatic image of slit 1 at slit 2. Spectrometer S2 plate separation was tapered so that the wide end was at the upstream end; the variation of plate separation was such that the beam level was raised about 0.1 inch. Slit 2 was 0.090 inch wide (vertically).

Quadrupole Q2 had little effect on the transmitted beam vertically; but, being divergent in this plane, it helped to bend the deflected lighter particles farther out of the horizontal plane. For the same reason the second slit was magnetized, with a small number of appropriate windings producing a horizontal field in the iron. In addition to the slits, vertical collimators were placed in Q1 and M4 (to prevent particles from spraying onto spectrometer plates and thus back toward the center of the channel) and also in M1, M2, Q3, and M6.

In both stages of separation, pions and muons were deflected upwards. In the first stage this deflection served to keep the lighter-particle image of the target holder (located below the target) from being superimposed on the first slit. Experience with the 1.15 BeV/c beam which deflected pions downward in the second stage, had indicated that pions entering the chamber tended to enter higher than K's.[1] Thus it was decided that both stages should deflect the lighter particles upwards for the K-72 beam.

III. DETAILED DESCRIPTION OF BEAM ELEMENTS

The over-all plan of the beam has been described. A diagram of the beam layout appears in Fig. 3, and a ray diagram of the optics in Fig. 7. In this section we consider the design of the individual elements of the beam.

A. Target and Front End Design

Two targets at different radii on a single "traveling" platform were used to obtain the variable beam momentum. Made of copper, they were 0.1 inch high, 0.25 inch wide (i.e., in the radial direction), and 4 inch long

(in the proton-beam direction). The height and width were determined by similar considerations: large enough to intercept most of the proton beam (after many excursions) when the target was flipped into it; and small enough (of same order as aberration effects) so that the images of the target would be small, as required for good K separation. Finally, considerations of production processes by the incident protons and subsequent absorption of the products within the target determined the optimum length. (Four inches of copper is about one mean free path for absorption of protons with 6-BeV energy.)

Only those particles leaving the target with production angle close to 0° were accepted by the beam channel. The yield in the forward direction for such a target, for negative pions with momenta in the region of 1 to 2 BeV/c, had been found in previous experiments[2] to be about 7×10^{4} pions/millisteradian/(1% dp/p)/10^{11} protons. The K to π ratio in this momentum region is about 7×10^{-3} at the target. The average internal proton beam intensity during this experiment was slightly less than 1×10^{11} protons/pulse. The momentum bite accepted by the beam channel collimation was 6%, and the solid angle was about 0.3 millisteradian (see Table I). Finally, the beam path length from target to chamber was 155 feet, which is 4.3 decay lengths for K's of 1.55 BeV/c. Thus at this momentum about 1.4% of the K's lived long enough to reach the chamber. These numbers yield an approximate value for the flux at the chamber of 14 K^- per pulse. However, there is some loss of K's in the beam-line and at the slits; about 10 K's is closer to a correct estimate at this momentum.

The targets, and the exit channel through the Bevatron magnet, were located in the northwest quadrant of the Bevatron. (See Fig. 8.) The reference point in the exit channel used in calculating target positioning and optics was at a radius of 720 inch from the center of the quadrant, and at an azimuth of 36.66° measured from the west end of the quadrant. Particles were to pass the reference point at an angle of 37.37° to the radial vector at that point. This required some steering by the magnet M1 (see below). With the above information as input, an IBM 650 program ETHELBERT* calculated the positioning and optics of the targets for various momenta. Results are shown in Table I. The targets could be moved azimuthally. The inboard target (R = 598.4 inch) was used at the higher momenta, the outboard (R = 600.4 inch) at the lower. The vertical position of the targets was 3/16 inch above the median plane of the Bevatron. Beam studies at the ends of the quadrant indicated that this was the optimum height for maximum interception of the proton beam in this region.

The return magnetic flux in the channel through the Bevatron yoke was too high for this experiment; it also had gradients which could cause serious aberrations of the target image. Therefore an iron shield was placed inside the vacuum tank coupling the Bevatron to the beam-line. This shield reduced the field and its non-uniformities to manageable proportions. However, running at various momenta with the same location and direction upon entering the first stage of the beam line) necessitated more than just a movable target.

---

*by Victor Brady, LRL. For snout magnetic-field information, see Kalbfleisch et al., Alvarez Physics Memo 272 (unpublished).

Table I. Parameters related to target positioning and optics.

Parameter	K^- Momenta 1.25 BeV/c	1.55 BeV/c	1.85 BeV/c
ϕ_{target}	23.94 deg	22.94 deg	21.73 deg
R_{target}	600 3/8 inch	600 3/8 inch	598 3/8 inch
Energy (incident protons)	5.74 BeV	6.21 BeV	6.21 BeV
Obj. distance[a] (real)	193.54 inch	201.75 inch	213.30 inch
Obj. distance[a] (horizontal, virtual)	606 inch	545 inch	610 inch
Obj. distance[a] (vertical, virtual)	156.2 inch	161.8 inch	170.1 inch
Magnification (vertical)	0.55	0.55	0.55
Acceptance (horizontal)[a]	43 mrad	39 mrad	34 mrad
Acceptance (vertical)[a]	9.0 mrad	8.6 mrad	8.3 mrad
Acceptance (total)[a]	0.38 msterad	0.33 msterad	0.28 msterad
% K's surviving at chamber	0.61%	1.37%	3.17%

[a]With respect to center of exit channel at $\phi = 36.66°$, R = 720 inch.

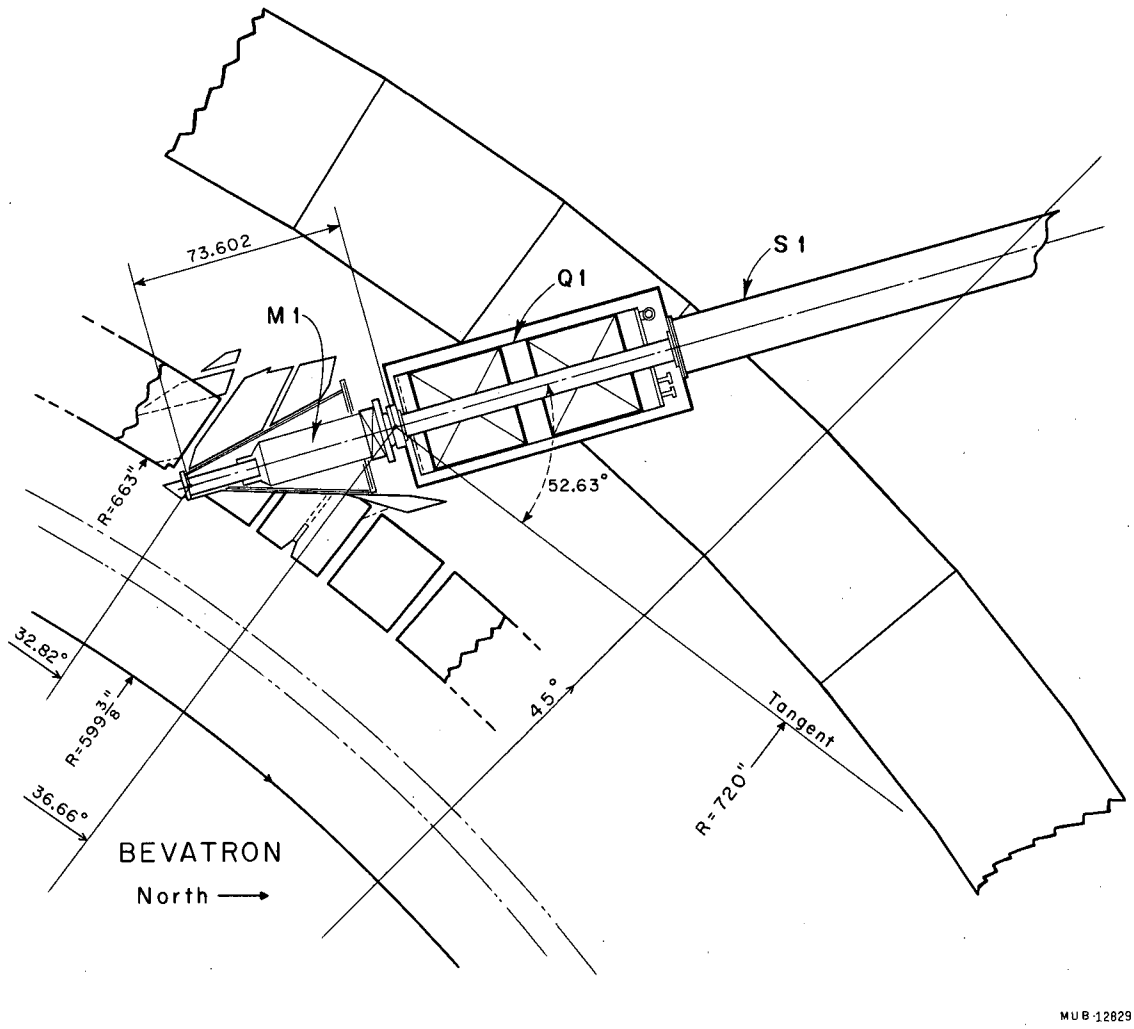

Fig. 8. The exit channel arrangement.

A steering magnet M1 specially designed for the experiment was situated inside the snout or yoke channel.* Figure 9 shows cross-section views of the shield and M1. Table II includes the currents and fields in M1 for several momenta. Placing the steering magnet within (rather than outside) the Bevatron yoke permitted a large momentum range, and a large solid angle, and prevented excessive length in the beam-transport system.

B. Spectrometers

The spectrometers were of the heated glass-cathode type developed by Murray.[3] Electromagnetic spectrometers are limited in field strength by sparking which occurs at high electrical fields. For metal electrodes in vacuum, separated by a gap of a few centimeters, the highest field obtainable without severe sparking is about 60 kV/cm. Use of a heated glass cathode and a small pressure (about 1 μ) of argon permits a field of about 90 kV/cm. Glass at 100° behaves as a conductor in the static region, so that the electric field is normal to its surface. However, its resistivity is high enough to inhibit a rapid build-up of charge in a small region, and thus damp or prevent those sparks which involve in their incipient stage an emission of electrons from a small area of the cathode. The 1μ of argon prevents ion-exchange processes between the electrodes which limit the voltage and damage the cathode. By what means the argon helps is not entirely clear.

Figure 10(a) shows an end view of the spectrometer electrode assembly. Figure 10(b) is a picture of the electrode structure. The outer structure was a 20-foot-long vacuum-tight iron box, containing current sheets in the top and bottom to generate a horizontal magnetic field; the side walls thus acted as pole faces. The anode was made of stainless steel sheet 0.063 inch thick, and was 6-3/4 inch wide and 230 inch long. Stainless steel pipe two inches in diameter was spot-welded around the sides and ends so that the plate was 1/8 inch below the top of the pipe. This served to eliminate sharp edges and to keep the field constant within 1% out to about 4 inch from the centerline. The cathode was made of soda-lime glass 1/2 inch thick, 10 inch wide, and 230 inch long. Heaters were installed along the enclosure corners nearest the cathode. A thin aluminum heat baffle helped to maintain the required 100°C temperature. Each spectrometer had a high-vacuum system that pumped out air (and admitted argon). To isolate the spectrometers from the rest of the beam line, 0.002 inch Mylar foil windows were installed at the ends. These had negligible effect on the virtual size of the target due to multiple scattering.

For reasons discussed in Sec. II, the electrodes were not quite parallel. The average gap was about 2 1/4 inch (with minimum separations of 2.0 inch and maximum separations of 2.75 inch and 2.30 inch). The performance of the spectrometers as determined by the spark rate varied with time, despite a long "bake-out" period. The voltage they could maintain was between 450 and 500 kV. The corresponding magnetic field was about 300 gauss.

---

*The entrance of the "29°snout" channel was widened by removing and trimming yoke laminations. Calculations of Glenn Lambertson were indispensable for this alteration and also for the design of the steering magnet.

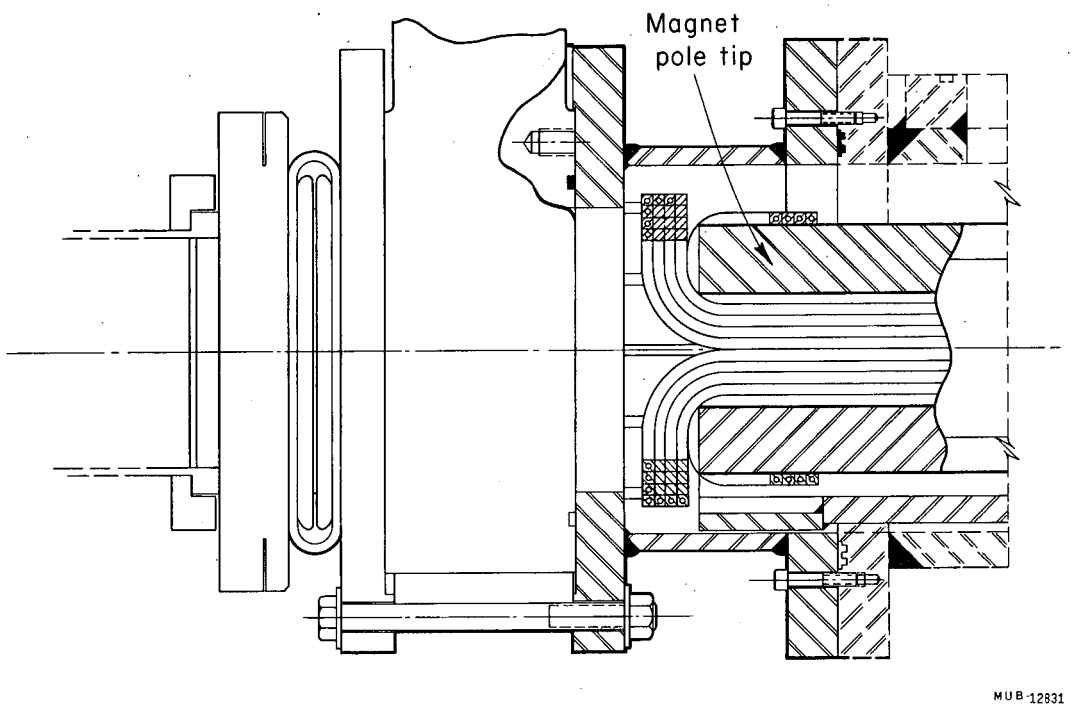

Fig. 9. Side view of downstream end of the steering magnet M and a portion of the vacuum tank. (Pole tips and tank walls are cross hatched. The 16 turns of copper coil around each pole tip are visible.)

Table II. Bending magnet fields and quadrupole field gradients at three representative momenta. The corresponding magnet currents are included also.

Magnet	Field or field gradient (kG or kG/in.)[a]			Current (A)		
	1.25 BeV/c	1.55 BeV/c	1.85 BeV/c	1.25 BeV/c	1.55 BeV/c	1.8 BeV/c
M1	-2.09	0 (or -0.55)[b]	2.02	-339	0 (or -89)[b]	327
$Q1_{F}$[c]	0.79	0.98	1.13	330	407	471
$Q1_{R}$[c]	0.72	0.90	1.04	301	375	435
M2	10.1	12.5	14.9	333	413	510
M3	10.1	12.5	14.9	713	663	828
Q2	0.78	0.96	1.18	338	420	516
M4	10.1	12.5	14.9	706	666	828
M5	10.1	12.5	14.9	321	400	489
$Q3_{E}$[c]	1.21	1.53	1.75	503	638	729
$Q3_{c}$[c]	1.19	1.49	1.72	498	621	717
M6	11.3	14.0	16.8	288	352	490
Q4	0	0.35	0.69	0	150	300

[a] kG for bending magnet fields; kG/in. for quadrupole field-gradients.

[b] Either target could be used at the central momentum. The zero setting corresponds to the outer (600 3/8 inch) target.

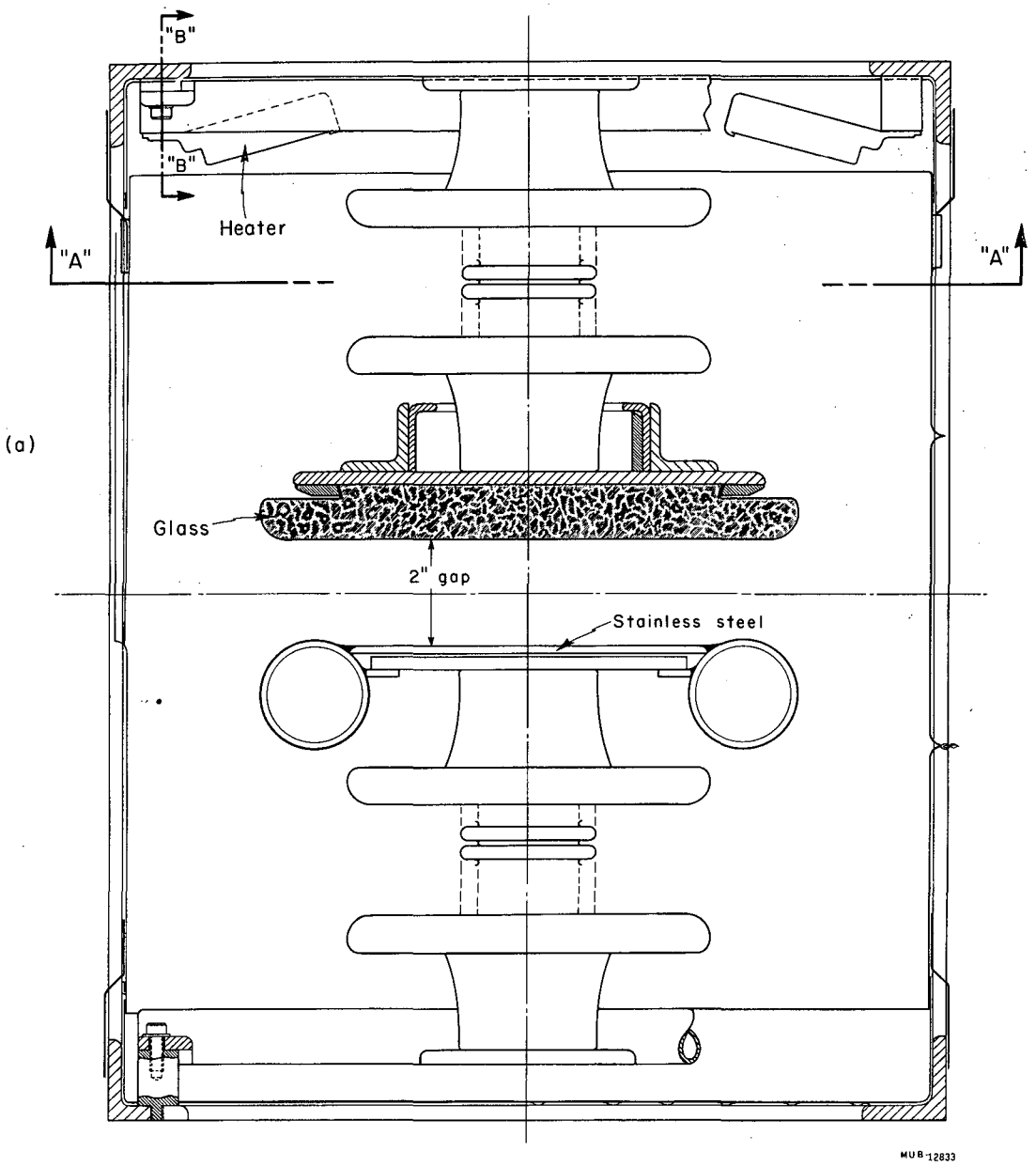

Fig. 10(a). End-view drawing of a spectrometer electrode assembly.

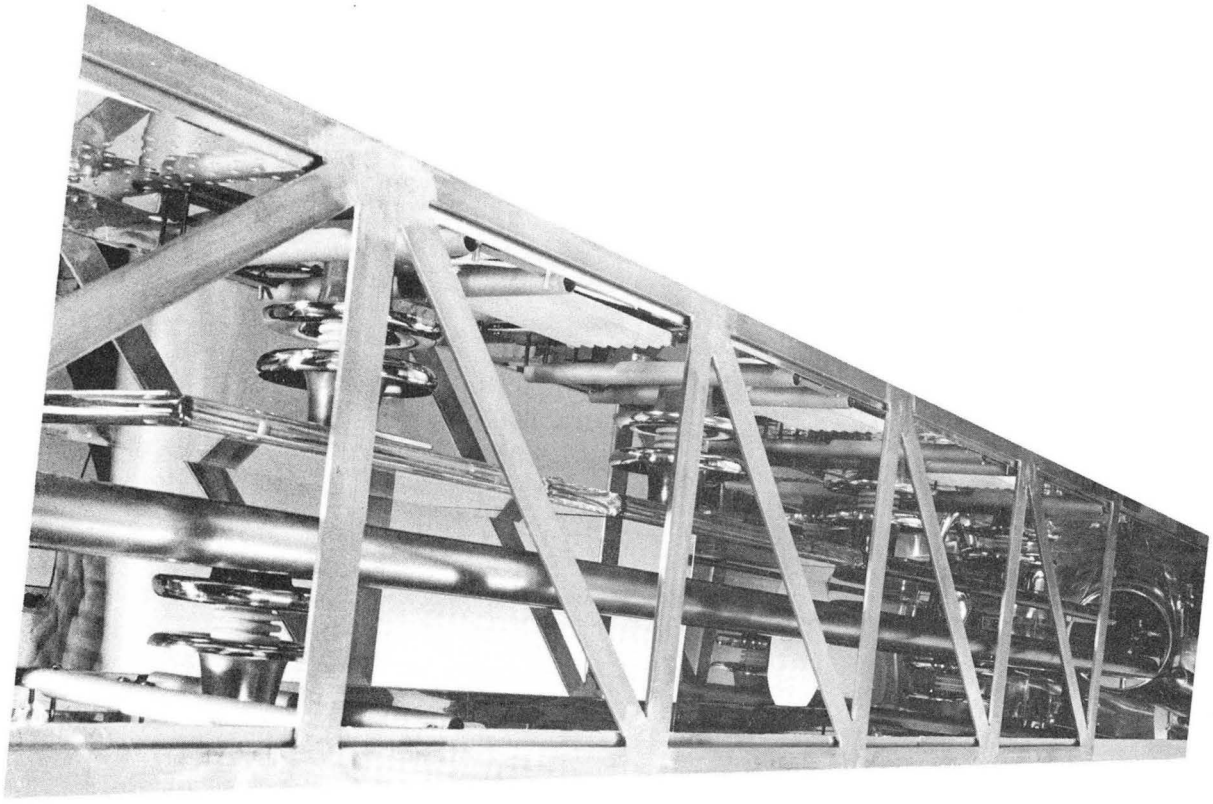

ZN-2639

Fig. 10(b). Picture of electrode structure.

C. Quadrupoles

The doublet quadrupole preceding the first spectrometer and the triplet quadrupole following the second spectrometer were both of 8-inch bore. In length the doublet sections measured 32 inches each, and the triplet sections were 16-32-16 inches. At 1.55 BeV/c, field gradients for the doublet were 980 and 900 kG/in. (for the end nearer the target and that nearer the spectrometer, respectively); for the symmetrically run triplet the gradient were 1460 kG/in. for the ends and 1490 kG/in. for the center. The resulting focal lengths in the vertical plane were 110 and 191 in., for the doublet and triplet, respectively. (See Table II.) The corresponding vertical object distances were 185 inch for the doublet and 169 inch for the triplet (measured from the center of the nearest magnet section); these were the distances from the vertical virtual target to the doublet upstream section and from the triplet downstream section to the second slit (see Fig. 6).

Wire-orbit studies were made of the quadrupoles at three different momenta (i.e., with the magnet currents suitable for these), 1.25, 1.55, and 1.85 BeV/c.[4] Measurements were carried out by adjusting the angle of an outgoing ray relative to one of the planes of symmetry to make the entry ray parallel to the quadrupole central axis. A transit sighting along the wire from a pulley to a cross-hair on the wire immediately before the magnet was used to determine parallelism at the entry end. A tie-point and an rf detecting head mounted on lathe-drive mechanisms were used to determine two points on the exit ray.[5] Focal lengths and principal planes were calculated for all quadrupole assemblies at each momentum. Also the perturbations in quadrupole currents needed to change the focusing in one plane without disturbing that in the other plane were determined. (This was done first by the use of IBM 650 computer programs DIPOLE and TRIPOLE,[6] and then checked with the wire-orbit technique.) Thus it was possible to construct a "current grid" to be used in actual beam tuning, with one family of curves for constant vertical object (doublet) or image (triplet) distances and the other family of curves for constant horizontal object or image distances. (See Fig. 11 for the doublet quadrupole. A similar current grid was constructed for the triplet quadrupole with end current plotted vs center current for various image distances.)

The wire-orbit measurements indicated that the quadrupoles could be assumed to be fairly linear in the region from 700 MeV/c to about 1.2 BeV/c; but at 1.55 and at 1.95 BeV/c, deviations from linearity became evident.

Extensive study by wire-orbit techniques showed that chromatic aberrations were very close to those expected, but that spherical aberrations were also present to an intolerable extent. Results of aberration studies for the uncorrected doublet quadrupole are shown in Figs. 12 and 13. Corrections for chromatic aberrations were made at the position of dispersed horizontal images, in the bending magnets; these are discussed elsewhere (Sec. III. D) in this article. Corrections for spherical aberrations were made by adding some iron at the edges of pole tips in certain quadrupole elements. This was accomplished by taping drill rods to the pole tips in the configuration shown in Fig. 14. (For the doublet, four pieces of drill rod 1/8-in. in diam by 28-in. long were used in the vertically diverging element; for the

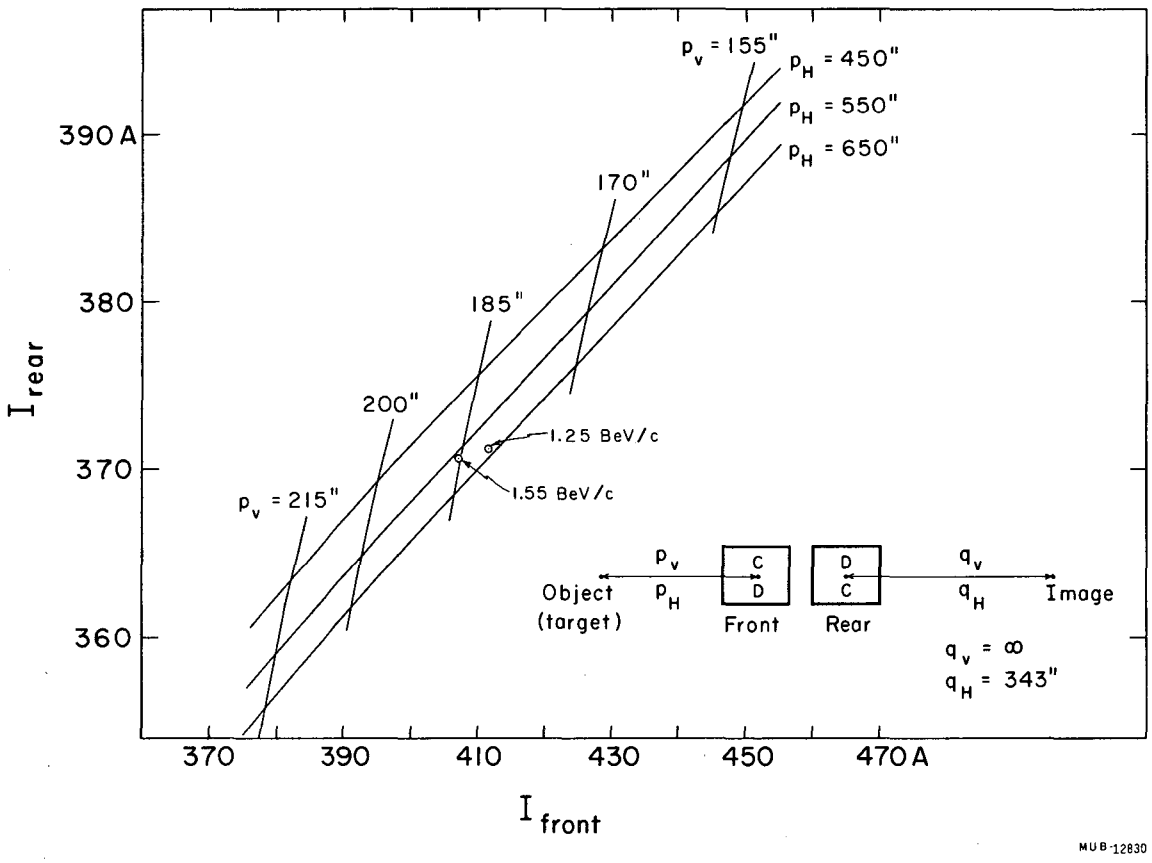

Fig. 11. Current grid prepared for tuning of the double quadrupole in the first stage; current in the front element (that nearer the Bevatron) is plotted versus current in the rear element. The families of curves are for various fixed object distances (to the virtual target) in the horizontal or vertical plane. Points labelled 1.25 and 1.55 BeV/c are the estimated operating points for those beam momenta.)

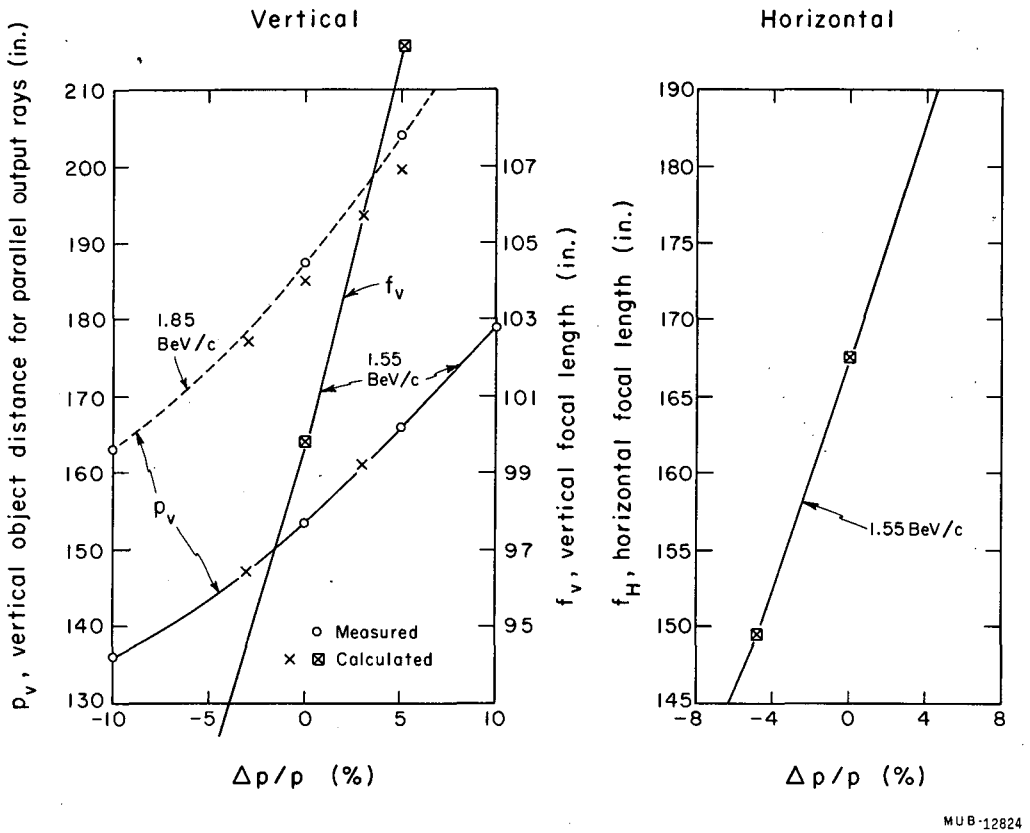

Fig. 12. Uncorrected chromatic aberration effects in focusing of the doublet quadrupole. The abscissa represents the fractional change in beam momentum.

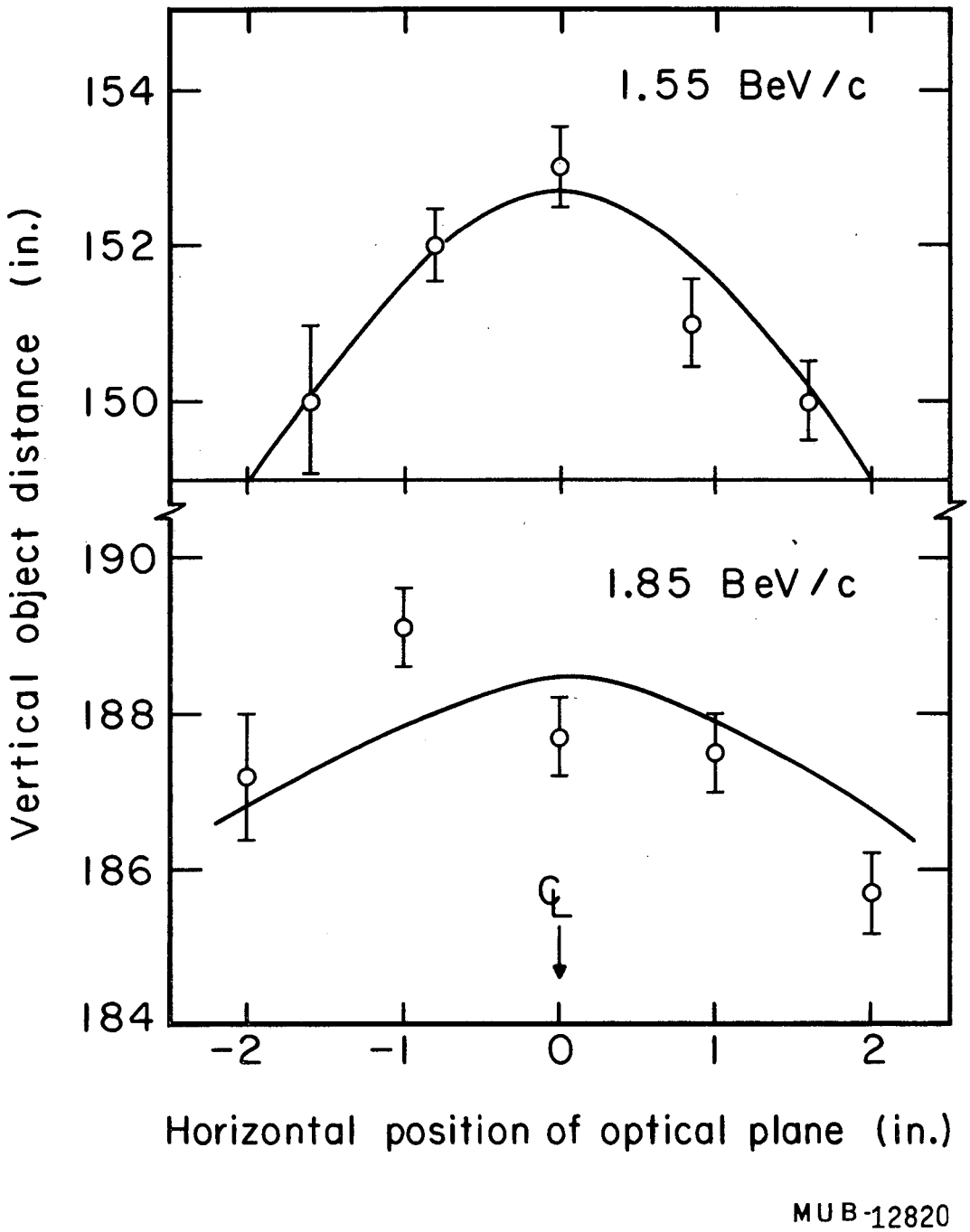

Fig. 13. Uncorrected spherical aberration effects in focusing of the doublet quadrupole. Variation of vertical object distance with horizontal displacement is shown. (Vertical "object distance" here is referred to the center of a quadrupole element, cf. Fig. 11. Output rays are parallel.)

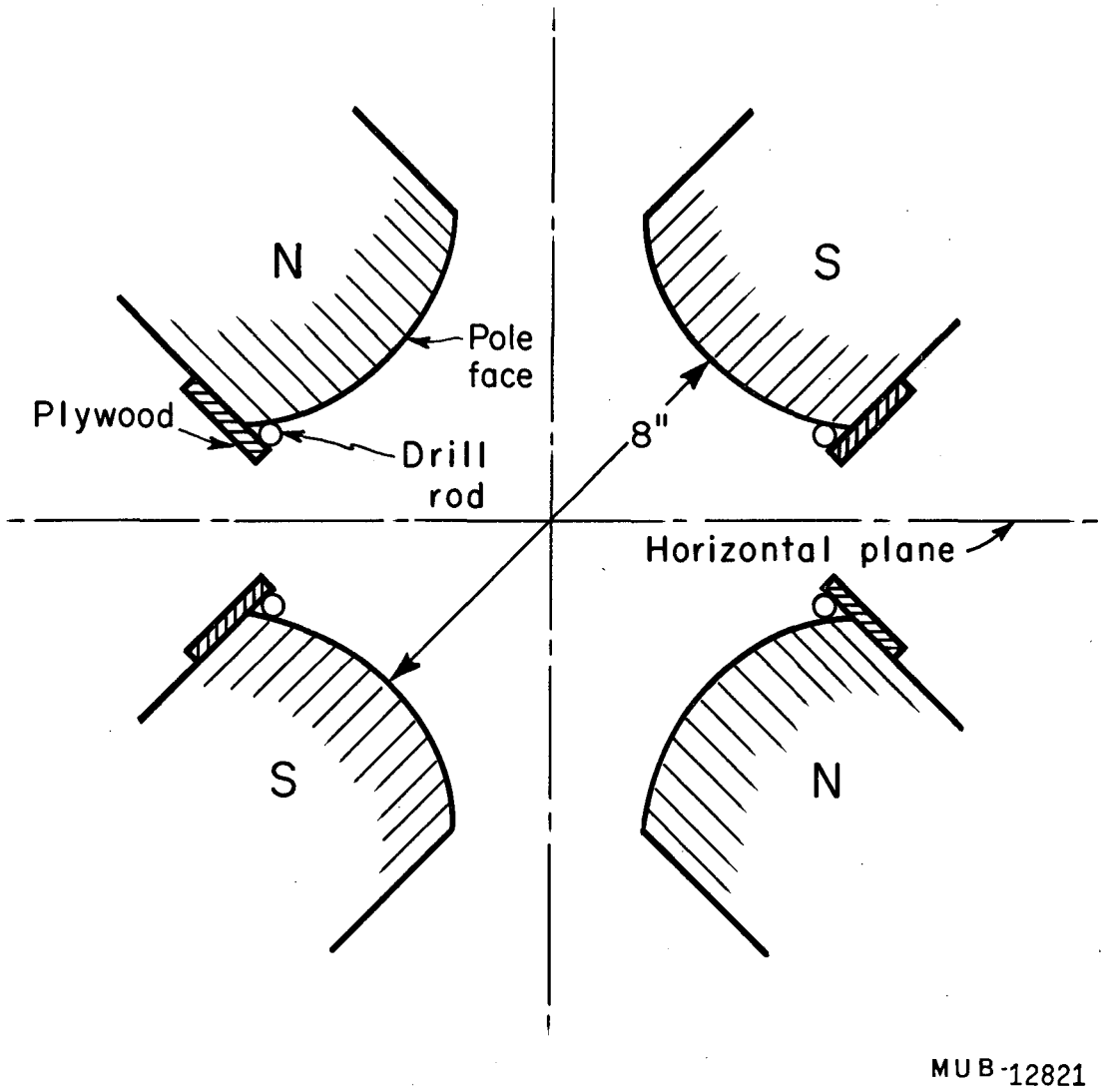

Fig. 14. End view of quadrupole pole tips showing configuration in which iron drill rods were placed for correction of spherical aberrations.

triplet, four pieces of rod 1/4-in. in diam by 10-in. long were used, again in a vertically diverging element.) The effect of the shims for the doublet and triplet quadrupoles is shown in Fig. 15.

An unanticipated source of difficulty in quadrupole focusing was an appreciable rotational misalignment of elements. Wire-orbit studies of the triplet quadrupole indicated that rays parallel to the horizontal plane were not focused (vertically) in the horizontal median plane, but in a plane tilted 0.12 radian (1/2 inch vertical displacement inch transverse displacement for the line of images!). Correcting one poorly aligned end section of the triplet by rotating pole-tips (after milling out bolt holes) 60 mils at a radius of 4 inch brought the image plane back to the horizontal.

An additional singlet quadrupole of 8-inch bore was used as a "field lens" at the first slit; horizontally it focused Bend 1 images onto Bend 2. Only a small amount of wire-orbit work was done on this quadrupole, namely, the determination of focal lengths for central rays at 1.25, 1.55, and 1.85 BeV/c. No shimming was done.

D. Bending Magnets

Perhaps the most important innovation in the design of the K-72 beam was the use of shimmed bending magnets to provide vertical focusing usually accomplished by quadrupoles and to compensate (by variation of the shimming across the bending magnet) for the chromatic aberrations of the Bevatron field and of the doublet and triplet quadrupoles. A further function of the bending magnets was to cancel approximately the dispersion of the Bevatron field and to permit the superposition of horizontal rays of all momentum components at the first slit.

The first and the second bends in the beam were symmetrically located with respect to the first mass slit, the first bend coming immediately before the second spectrometer. Each bend was 31 deg in magnitude, with the second bend opposite in direction to the first. A pair of magnets was necessary to produce each 31-deg bend at momenta as high as 1.85 (and later 1.95) BeV/c. A low-power "H-magnet" and a "C-magnet" were used in combination, with the H magnet run at about 12.5 kG (407A) and the C magnet also run at about 12.5 kG (704 A) for the 1.55 BeV/c momentum.[7] The two magnets were supported on one long concrete block; their relative positions were fixed by putting under both magnets a large 3/4 inch thick iron plate which had holes for dowel pins fixed to the magnets. A rather large box was welded into the beam vacuum-pipe system between the H and C magnets; inside the vacuum box there were massive (about 12-inch long) copper "jaws" which could be closed or opened from outside the vacuum box to permit selection of a certain momentum bite. The "low-momentum" or -3% component of the beam was focused horizontally at the outside of each bend (in the H magnet); the 0% component was focused at the center (between H and C magnets); and the +3% component was focused at the inside of the bends (in the C magnet). (See Fig. 16.)

Both magnetic shims and current windings were necessary for the bending magnets; the former accomplished the correction of field gradient needed at 1.55 BeV/c, while the current loops provided the trimming necessary for other momenta.

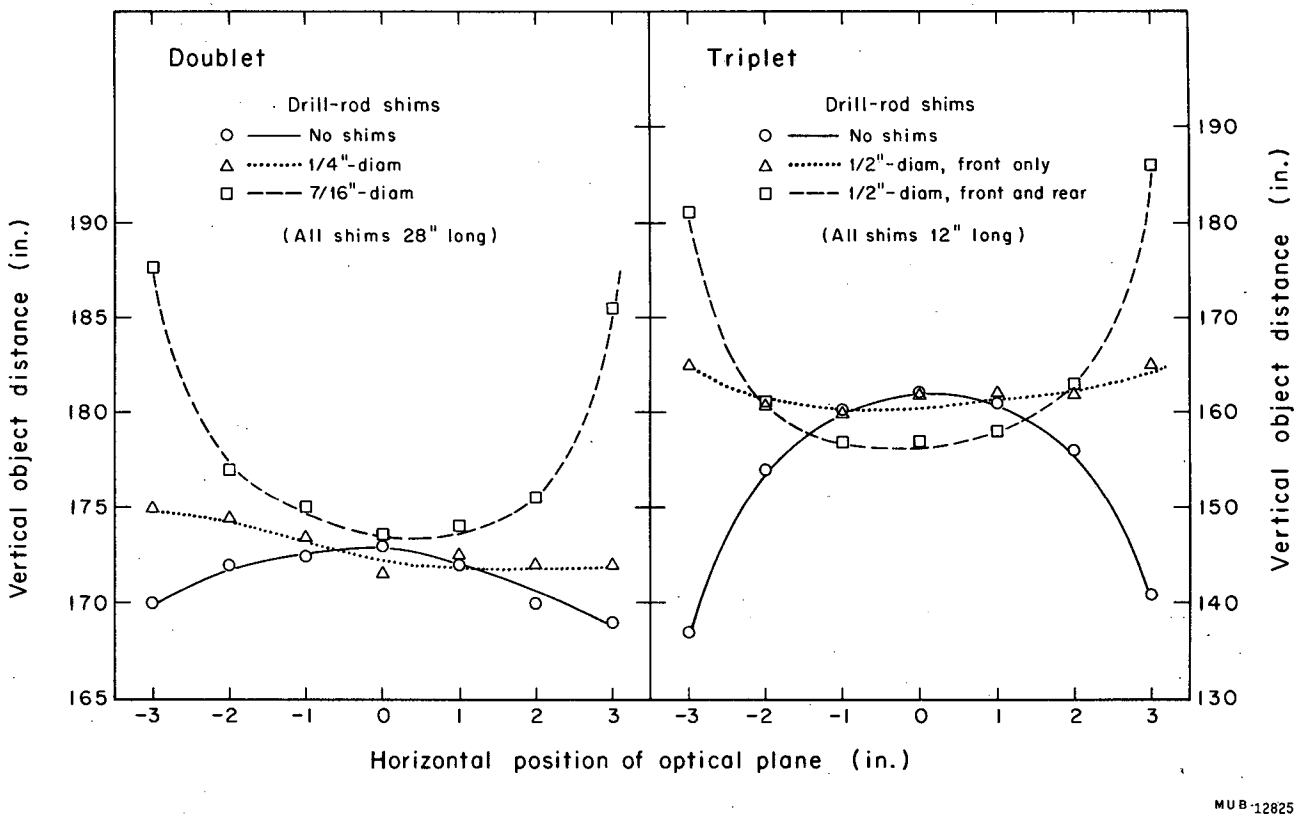

Fig. 15. Correction of spherical aberration effects in doublet and triplet quadrupoles. The sizes of iron rods described in the legends produced the indicated change in vertical focusing; the corrective rods selected were those giving most nearly constant vertical focusing across the doublet and triplet quadrupoles.

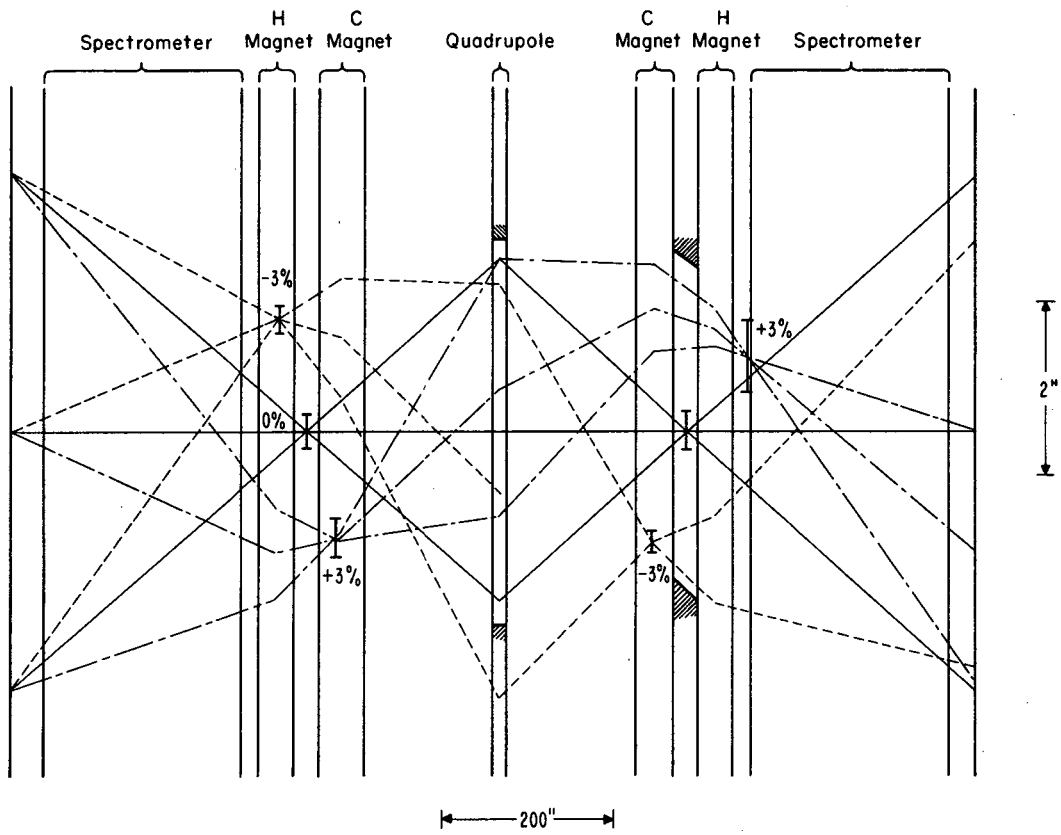

Fig. 16. Horizontal-ray trace through central portion of beam. The extremes of momenta ($\Delta p/p = \pm 3\%$) as well as the central momentum are shown. ---, $\Delta p/p = -3\%$; —, $\Delta p/p = 0$; — — —, $\Delta p/p = +3\%$; $p = 1.55$ BeV/c.

The gap height in the bending magnets without shims measured 6-1/4 inch. Each of the two packages of magnetic shims required about 1/4 inch of vertical space inside the top and bottom pole tips. Finally each set of 1/4-inch high (with insulation) pole-tip windings was mounted on a 1/4-inch thick aluminum plate; the plate-winding assembly was bolted onto each pole tip through clearance holes in the magnet shim package. Space left for the vacuum tank measured 4-3/4 inch vertically.

In the vertical plane, the low component of momentum was converging in the separator (to an image 1200 inch beyond the center of the bend); the "on-momentum" component was parallel (or focused at infinity); and the high-momentum component was diverging (with a virtual image 2000 inch before the center of the bend). (Description is in terms of the optics of the first stage.) The special shimming of the bending magnets was to bring all these momenta to the same vertical focus 217 inch beyond the center of the bend. Hence considerable variation in shimming across the magnet was needed. To determine the necessary correction, flux-coil measurements were used to find the transverse gradient of field integrated along beam line. It was found convenient to plot the quantity $(f_v \theta)^{-1}$ (directly dependent on this integral of the gradient) as a function of transverse position. Parameters such as f_v and θ are defined in Fig. 17, and discussed more thoroughly in the Appendix. Figure 18 shows the unshimmed result and the correction necessary to obtain the desired results.

The "staggering" of the horizontal images permitted most of the low-momentum shimming to be done in the H magnet and most of the high-momentum shimming to be done in the C magnet. Magnetic shims were made of stock 30 or 48 mils thick cut in strips which followed the contour of the beam through one magnet. These were stacked (with double-faced tape between layers) in sandwiches which were bolted directly onto the pole tip of the magnet. Typical "sandwiches" are shown in Fig. 19. Some corrections were also made with "end shims", i.e., blocks of iron bolted onto the vertical face of the end of the pole tip; these were simpler to arrange than the pole-tip shim layers. A current "sheet" was provided by passing copper windings (water cooled) along the pole tip; these followed the beam contour and were spaced about 1/2 in to 3/4 inch apart. The copper was a 0.2- by-0.2 inch hollow conductor; about 50 windings were on the top pole tip and 50 windings on the bottom, and each of these could carry current in a positive or a negative direction. A typical current arrangement is shown in Fig. 20 for 1.85 BeV/c. For a brief discussion of theory and for further experimental details on the shimming of the bending magnets, see the Appendix.

"Good guesses" were made on the forms of the required shims by determining the focusing effects of a unit magnetic shim and of one current winding. However, very extensive wire-orbit work was necessary to produce a satisfactory end result. Vertical focusing was studied for actual "extreme" and "central rays" or the horizontal-ray diagram with the wire-orbit technique. The radius of the circles of confusion at the slit 1 focus was finally reduced to less that 20 mils in most cases.

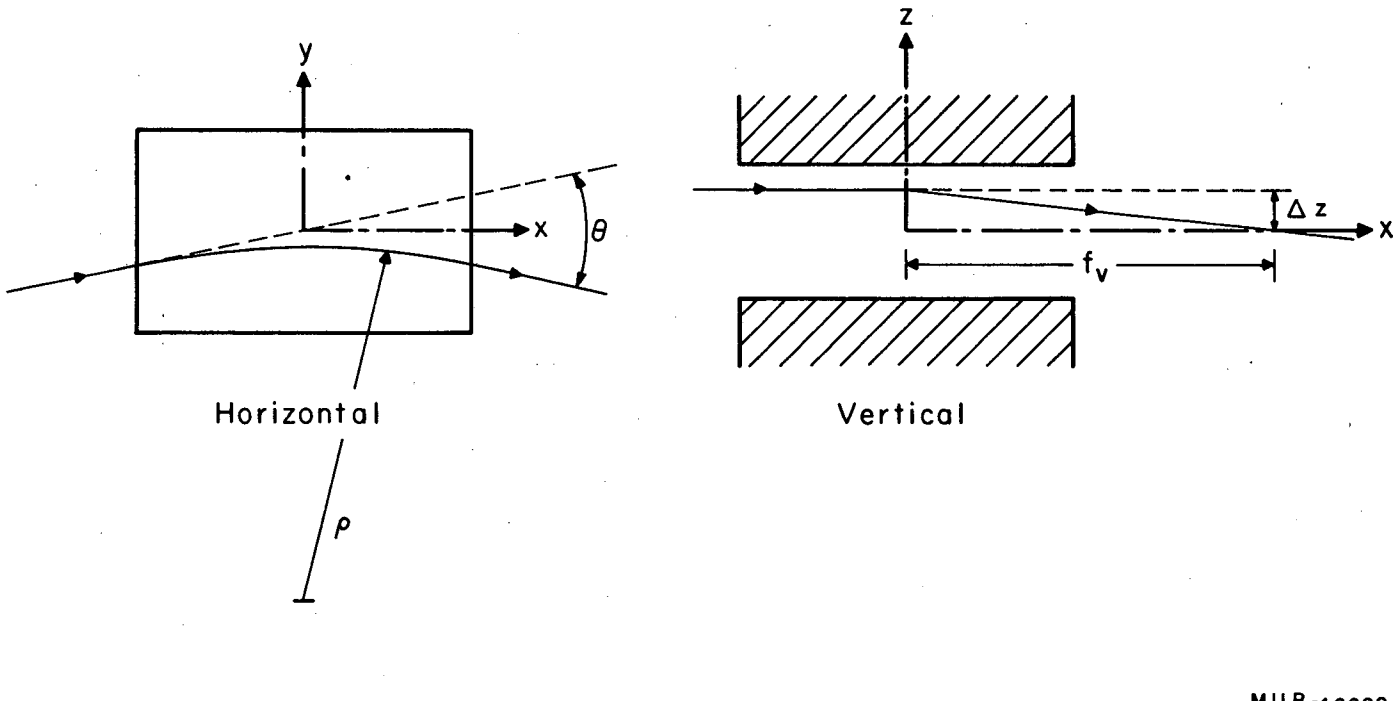

Fig. 17. Geometry of vertical focusing in bending magnets. The f_v is determined by ρ and θ.

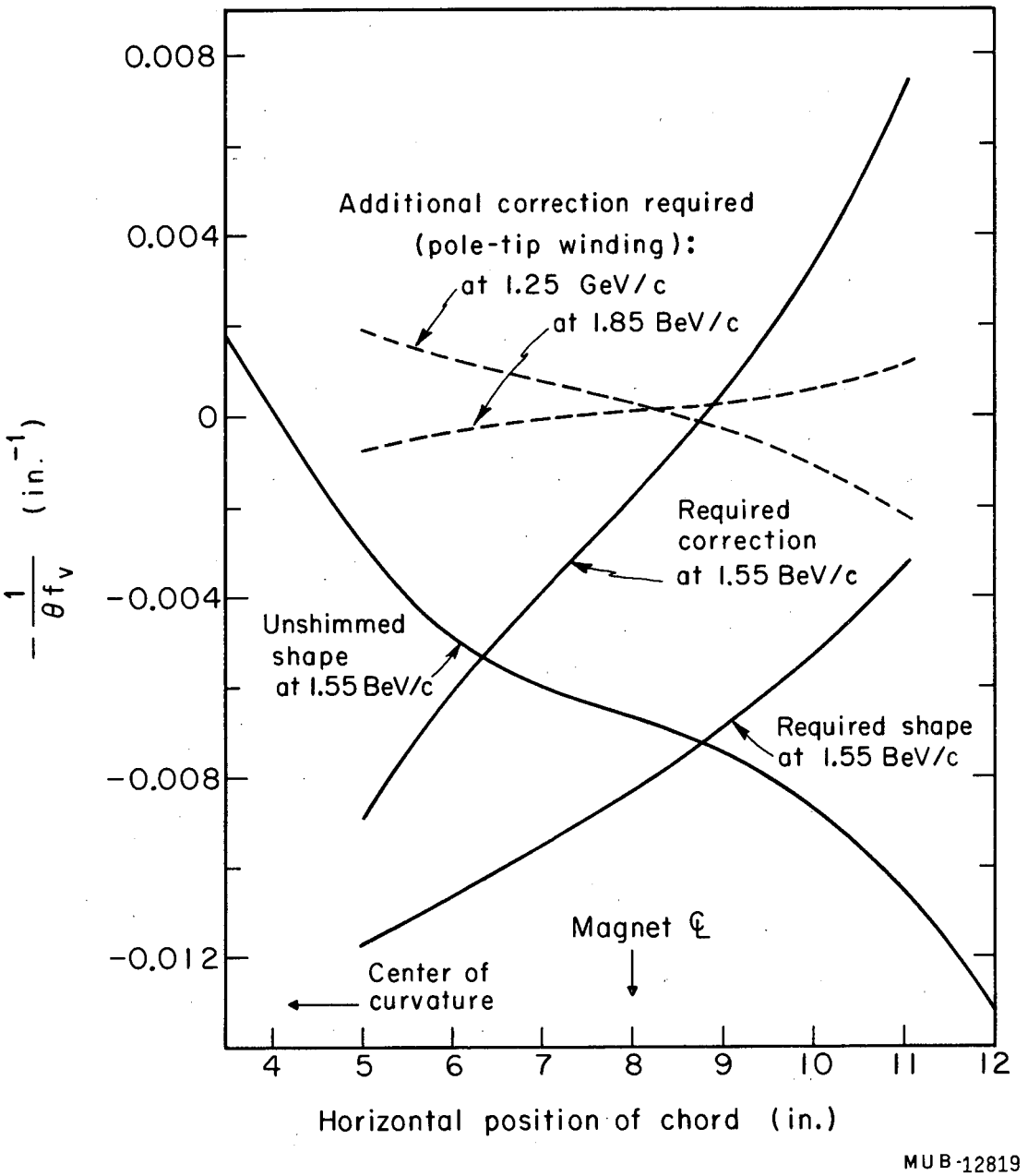

Fig. 18. Variation of the reciprocal of vertical focal lengths (times the bending angle θ) across the combination of C and H magnets used for one bend. Uncorrected vertical focusing and the desired end result of shimming are shown. (See the Appendix.)

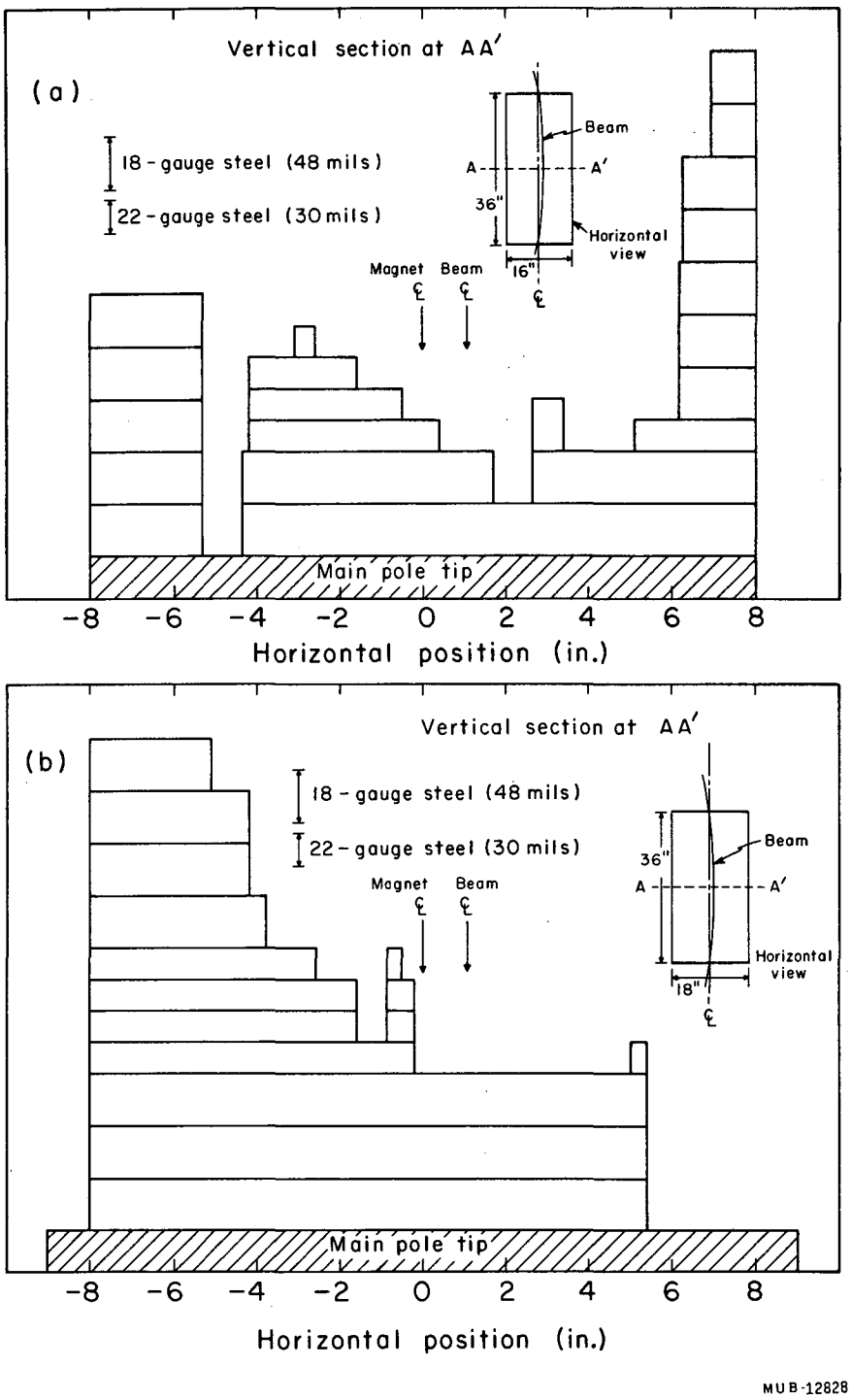

Fig. 19. Typical package of magnetic shims used for each of four bending magnets. (a) One C magnet; (b) one H magnet.

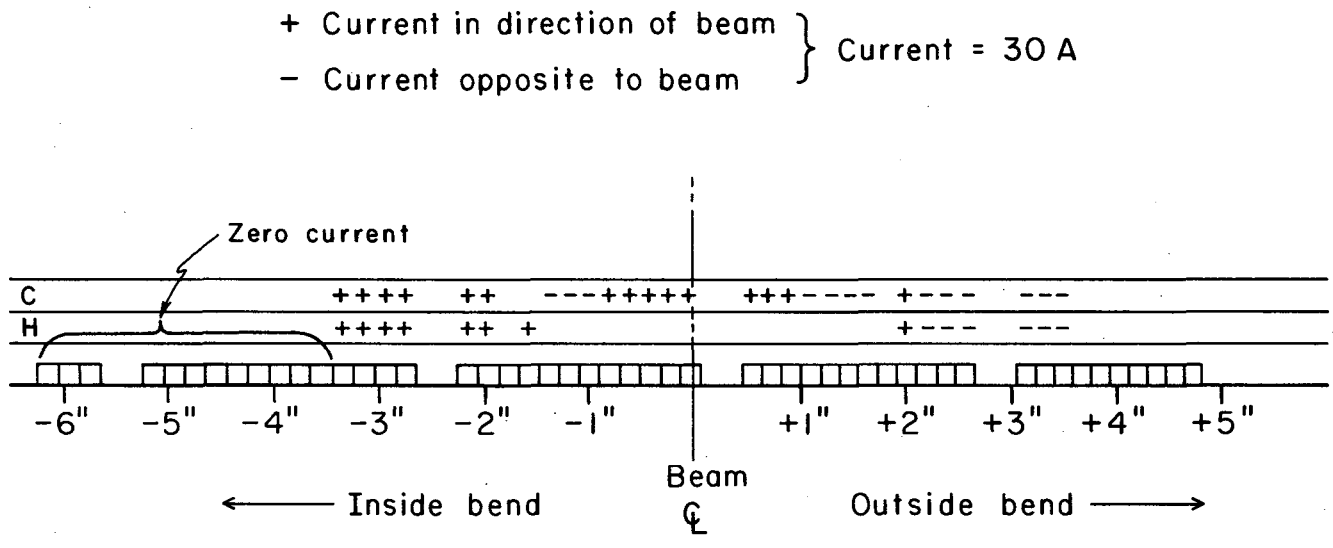

Fig. 20. Arrangement of pole-face currents (for 1.85 BeV/c) typical of those which gave desired corrective effects, in addition to corrections by the magnetic shims, for beam momenta other than 1.55 BeV/c.

IV. TUNE-UP, RUNNING, AND RESULTS

A Cerenkov counter and a telescope consisting of two scintillation counters were placed as beam monitors just outside a slot through the Bevatron magnetic yoke and shielding wall at an azimuth of 30° (upstream from the main beam channel). (See Fig. 8.) These counters were aligned to receive low-momentum secondaries produced in the target. The absolute rate of counting gave a measure of the flux entering the primary beam channel; the ratio of this rate to the circulating proton beam intensity indicated the efficiency of hitting the target with the protons--information of aid to the Bevatron main control room. These data were continually monitored.

The accurate positioning and alignment of the elements of the beam were crucial for its success. The various magnets and spectrometers were carefully surveyed into place. Slight final adjustments of some of the elements were made on the basis of the tuning procedure described below.

The horizontal optics were tuned first, with the spectrometers off, by means of a telescope consisting of three scintillation counters to measure the π flux produced by a low-intensity, $\approx$1-msec spill on target. The first two counters were 2 1/2 inch high, 8 inch wide and 1/2 inch thick. When placed at one of the slit positions they intercepted the entire beam. The third counter was 4 inch high, 1/2 inch wide, and 1/4 inch thick. A horizontal beam profile was obtained by moving this counter across the beam and measuring the coincidence rate. A rough tuning of the vertical optics was done with the third counter turned to be 1/4 inch high, 4 inch wide, and 1/2 inch deep. The above procedure was followed at both slits, with the jaws in the bending magnet pairs wide open. Then with the jaws narrowed to select smaller momentum intervals, the finer details of the horizontal focusing and spatial dispersion of momentum components were investigated. (A coincidence counter with small scintillator inside the vacuum tank superseded the jaws for this study; closed jaws caused severe scattering.) Figure 21 shows some horizontal profiles at the first slit. Figure 22 shows the relative flux intensities vs momentum at the entrance to the bubble chamber at several central momenta. The exact target azimuth required for acceptance of particles produced at 0° was determined by analysis with M5 of the beam's central momentum (with Q3 turned off); the bending angle (and thus the M5 current) required to center the beam at the second slit was a minimum for 0° acceptance. All properties of the beam were in close accord with the theoretical predictions.

Vertical steering was done with the magnetic field of the spectrometers. Some vertical profiles are shown in Fig. 23. With H_0 the field required to transmit the π beam through the slit with no voltage on the spectrometer planes, and H_π the corresponding field with the operating voltage applied, the field needed to transmit the K^- beam was $(H_K - H_0) = \beta_\pi/\beta_K \times (H_\pi - H_0)$, where the β's are the respective velocities. (This was slightly complicated by the non-uniform separation of the spectrometer plates.)

The vertical alignment was maintained with a scintillator counter sandwich ("triad") placed in front of each slit and mounted on a milling head. This consisted of three counters 1/16 inch high, 3 inch wide, and 1/2 inch thick. The signals from each triad were displayed consecutively on an oscilloscope trace so that when the π beam was centered on a sandwich, the

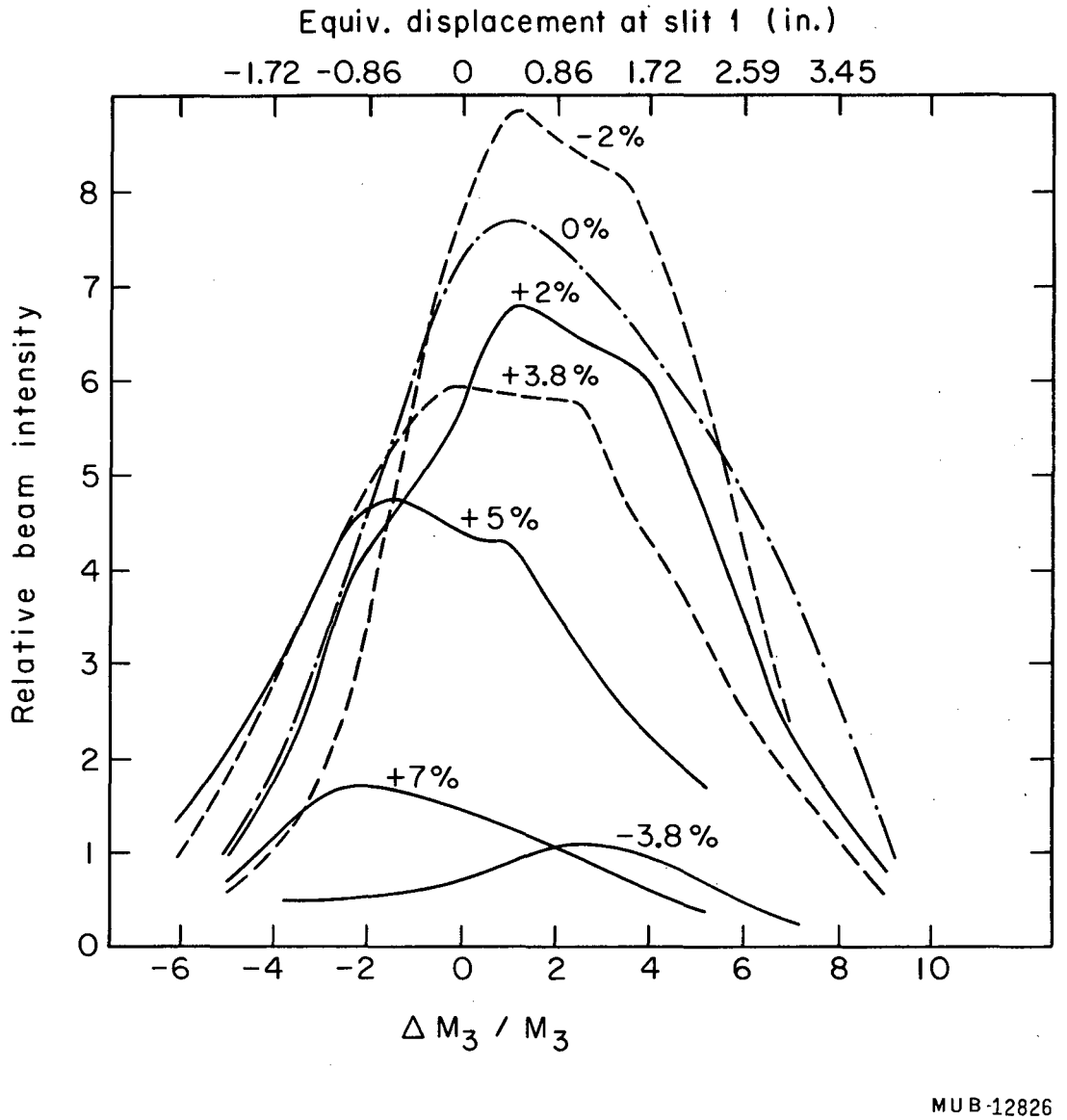

Fig. 21. Horizontal profiles of the pion image at the first slit for various momentum bites around the central momentum of 1.25 BeV/c. Momentum was defined by a 1/2-in.-wide counter in first bend.

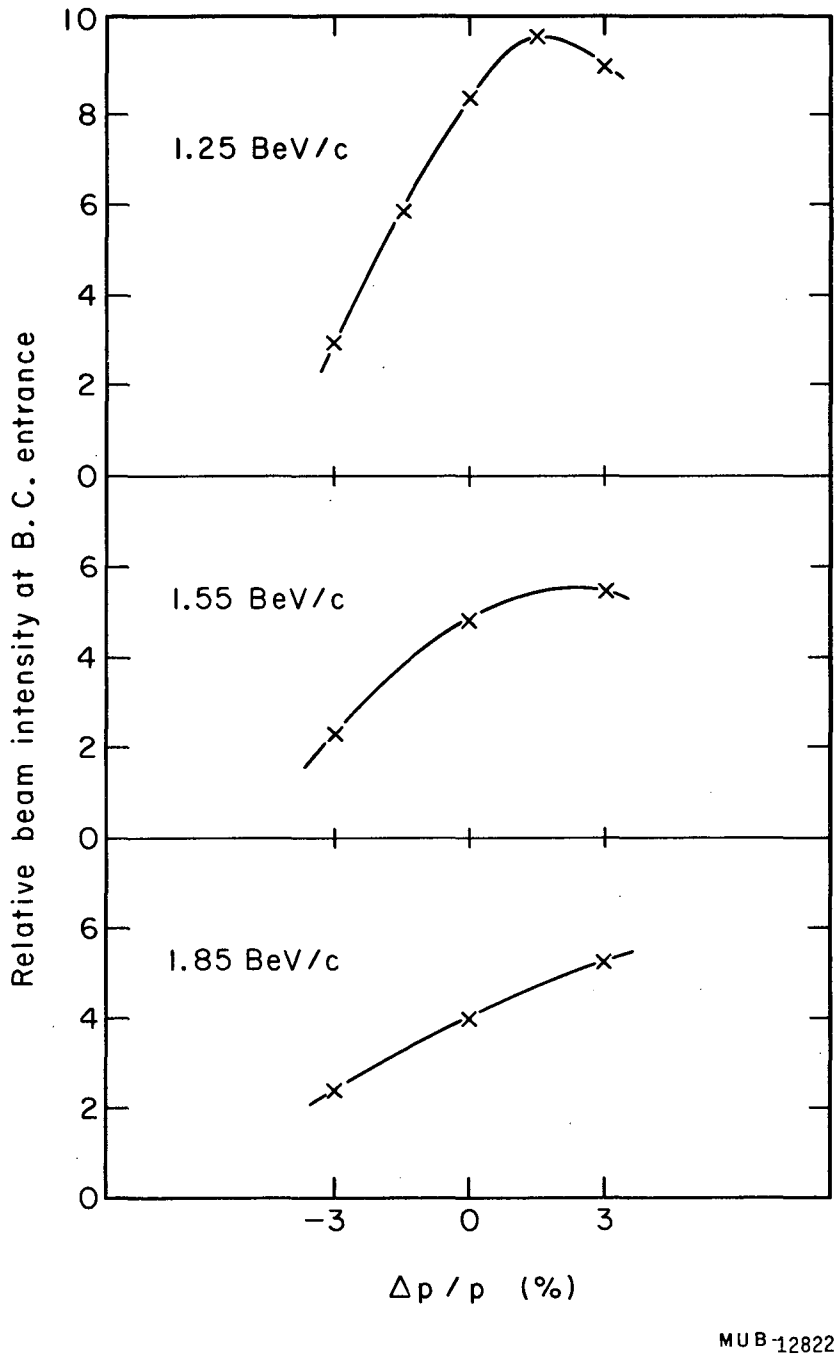

Fig. 22. Relative beam intensities at the entrance to the bubble chamber vs fractional change in momentum at central momenta of 1.25, 1.55, and 1.85 BeV/c.

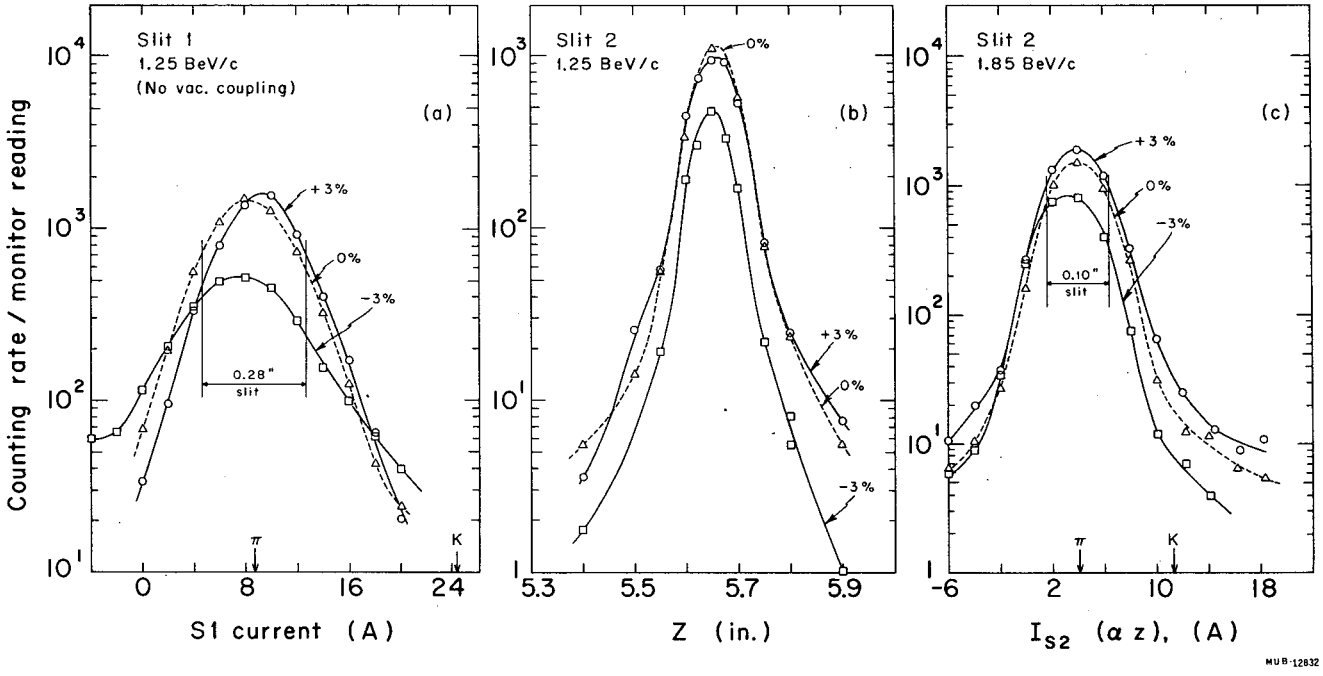

Fig. 23(a) and (b). Vertical profiles of the pion image at the first and second slits at 1.25 BeV/c. Electric fields for plots of Fig. 23 are zero, so magnetic current is small. With high fields, a K peak would appear at about 16A (or ≈ 0.55) higher than the π peak; also the images for ± 3% and 0% momentum of Fig. 23(a) would coalesce. These were taken before vacuum coupling of the Bevatron to the beam-line variable was available, so the images are slightly widened by the multiple scattering in the thin windows to the Bevatron and first stage. (Running at higher momenta was deferred until the vacuum coupling was available.) (c). Vertical profile at the second slit with beam momentum at 1.85 BeV/c. At high fields, a K peak appears about 7A above the π peak, and different momenta coalesce.

outer counters gave equally high spikes, with peak amplitudes in the middle counter. After a triad was centered on the transmitted pion beam (hence on the slit), it was moved up to the calculated position of the π beam rejected when the spectrometer was reset to transmit K's. This then acted as a sensitive monitor of the vertical steering. Periodic adjustments as indicated by the scope traces were made by varying the spectrometer magnetic fields.

The exposure of the bubble chamber lasted from September 1961 until June 1962. The experiment alternated with other activities at the Bevatron. In addition to running as planned at interval between 1.25 and 1.95 BeV/c, small K^- exposures were taken at 1.05 and 1.11 BeV/c. These momenta were obtained with the beam set for 1.25 BeV/c and a few inches of copper placed directly in front of the chamber. The loss of flux due to absorption in the copper was not quite as large as it would have been due to increased decay in the beam-line if the beam elements had been tuned down.

Running was done in hydrogen, and at some of the momenta, in deuterium. The magnitudes of the exposures are given in Table III, together with the estimated π and μ contaminations. (The μ contamination is not very serious since the μ does not interact strongly, and normalization is done on the basis of topologies unique to the K decay, not by numbers of tracks.)

Finally, it was often possible to run π's "parasitically" while other experiments were in progress because the large available π yield required that only a small percent of the circulating protons strike the target. Furthermore since separation was no longer a problem, the spectrometer limitations were inconsequential, and somewhat higher momenta could be obtained.

Table III. Magnitude of the exposures and estimated pion and muon contaminations at the various momenta.

Nominal momentum at chamber entrance (BeV/c)	Actual momentum at chamber center (BeV/c)	Hydrogen exposure (events/mb)	Deuterium exposure (events/mb)	Pion contamination (%)	Muon contamination (%)
1.05	1.04	200	---	a	a
1.11	1.11	100	---	a	a
1.25	1.22	1300	---	9	8
1.35	1.32	1410	---	2	5
1.45	1.42	850	---	4	3
1.55	1.51	5100	1040	4	0
1.65	1.60	760	---	2	2
1.75	1.70	1135	---	9	0
1.85	1.80	1100	---	a	a
1.95	1.90	1100	---	a	a

a. Undetermined or unknown.

APPENDIX: Vertical Focusing of Bending Magnets

Theory

In the approximation of small angles, the vertical focal length of a bending magnet can be found from the expression

$$(f_v)^{-1} = -(z)^{-1}\left(\frac{\Delta pz}{pz}\right) = -(pz)^{-1}\int q\,(\vec{v}\times\vec{B})_z\,dt = -q\,(pz)^{-1}\int (B_y dx - B_x dy)$$

where f_v represents the vertical focal length, p represents the momentum of the beam, and the coordinate system is that shown in Fig. 16. Taking only the first term of the Taylor's series expansion about z = 0 for B_x and B_y, and using the fact that the curl of B is zero, one obtains

$$(f_v)^{-1} = q(p)^{-1}\int_{-\infty}^{\infty}\left\{\frac{\partial B_z}{\partial x}\Big|_{z=0}\cdot\frac{dy}{dx} - \frac{\partial B_z}{\partial y}\Big|_{z=0}\right\}dx.$$

Since the bending angle θ is

$$\frac{q}{p}\int B_z\,d\ell,$$

this is equivalent to

$$(f_v\theta)^{-1} = (\int B_z d\ell)^{-1}\int_{-\infty}^{\infty}\left\{\frac{\partial B_z}{\partial x}\Big|_{z=0}\cdot\frac{dy}{dx} - \frac{\partial B_z}{\partial y}\Big|_{z=0}\right\}dx.$$

Expansion of the derivatives in the integral above as functions of y is necessary since the beam follows a curved trajectory and the magnet in general does not have gradients of field which are independent of y. After integration by parts and the elimination of insignificant terms, the integral becomes

$$(f_v\theta)^{-1} = (\int B_z d\ell)^{-1}\left\{\int_{-\infty}^{\infty}\frac{\partial B_z}{\partial x}\Big|_{y=z=0}\cdot\frac{dy}{dx}\cdot dx - \int_{-\infty}^{\infty}\frac{\partial B_x}{\partial y}\Big|_{z=0}\cdot dx\right\}.$$

The first part of the integral is rather insensitive to lateral displacements, as the horizontal focusing is too weak to cause dy/dx to change significantly for trajectories differing from the central trajectory; further, since the gradient dB_z/dx is large only in the fringe-field regions where dy/dx is close to the asymptotic value for the beam, the first term can be expressed as $(\theta f_{vo})^{-1}$, where f_{vo} is the usual expression for vertical fringe-field focusing, $f_{vo} = \rho_0/2\tan\alpha$. [Here, however, the finite extent of the fringe field should be taken into account by using an effective entrance or exit angle for α rather than the asymptotic value of $\theta/2$ in Fig. 17. An approximate expression for the fractional difference between the effective and asymptotic values of the angle α is (5/8)× gap/effective length of the magnet.]

Evidently the horizontal variation of the vertical focal lengths is contained entirely in the second term $\int_{-\infty}^{\infty} \frac{\partial B_z}{\partial y}\Big|_{z=0} dx$. Thus the measurement of the dB_z/dy gradient at the median plane integrated along the beam trajectory was required to determine the magnet's natural focusing properties; and magnetic shimming to change this gradient was needed to produce the desired focusing properties.

Experiment-Shimming

An estimate was made of the horizontally invariant vertical focusing term $(\theta f_{vo})^{-1}$ for a pair of magnets, each of which produced a bend of 15.5 deg; with an effective entrance and exit angle of 7.06 deg (rather than the asymptotic value of 7.75 deg), the estimate was

$$(\theta f_{vo})^{-1} = \frac{2 \tan 7.06°}{0.271 \times 155} = 5.9 \times 10^{-3} \text{ in.}^{-1}.$$

The second term, $\int_{-\infty}^{\infty} \frac{\partial B_z}{\partial y}\Big|_{z=0} dx$, was evaluated for various horizontal positions across the magnet by the use of a flux coil following the actual beam trajectory. The coil was moved in one-inch steps and the change in enclosed flux determined. From these results on the unshimmed magnet, the curve of Fig. 17 was obtained. (The quantity plotted is actually the average of H-magnet and C-magnet results. Further it was obtained with a bending angle of 38.5° rather than the 31° used in the final beam design.) Also shown in Fig. 17 are the required results and the necessary corrections, including the final corrections necessary for beam momentum changes from 1.55 to 1.25 or 1.85 BeV/c. The latter were to be made with the current windings to obviate the difficulty of changing iron shims after the installation of vacuum pipes. A study was made of the effect of a one-inch wide, 30-mil thick shim (one attached to each pole-tip in symmetrical locations) following the beam contour. On the basis of the flux-coil measurement of the focal effects of this "unit" shim, and also of the effects of simple combinations of unit shims, a package of shims was designed to make the necessary large corrections to the vertical focusing across the magnets. Wire-orbit studies were made of the shim package (shown in Fig. 18) and deviations from the desired end results were thus determined. Another modified shim package was then fabricated, and this was studied with wire-orbit techniques. As mentioned in Sec. III. D, end shims were used in addition to pole-tip shims to make the final adjustments.

The pole-tip windings found necessary to correct for magnet nonlinearities consisted of 50 copper wires (≈0.2 by 0.2 in. in cross section) run along each pole tip; the wires followed the contour of the beam and almost completely covered the effective pole-tip area of the magnet (-5 in. to +5 in. from beam center-line). A study of the focusing effects of four neighboring wires carrying 60 amperes each (in the same direction) was made, and from this the effects of simple combinations of positive-current and negative-current conductors were estimated. The final current configurations were decided on through wire-orbit studies. (See Fig. 19 for a typical current arrangement.)

ACKNOWLEDGMENTS

The encouragement and assistance of Professor Luis W. Alvarez, as well as the help of Robert Watt and his bubble chamber crew members, was much appreciated. James Brannigan contributed substantial help in beam construction, as did also George Edwards. The aid of the Bevatron staff members also was indispensable.

FOOTNOTES AND REFERENCES

1. Philippe Eberhard, Myron L. Good, and Harold K. Ticho, Rev. Sci. Instr. 31, 1054 (1960).

2. S. Goldhaber, Summary of Secondary Beams Produced at the Bevatron, BeV-493 Rev., March 1960.

3. Joseph J. Murray, Glass Cathodes in Vacuum-Insulated High-Voltage Systems, UCRL-9506, September 1960.

4. Wire-orbit study means the use of a wire carrying direct current to simulate a beam of rapidly moving charged particles. It is easy to show that T/I is proportional to the momentum of the beam, where T represents the tension exerted on the ends of the wire and I represents the current. [The exact relationship is p(MeV/c) = 2.94 T(g)/I(amp).]

5. The rf detecting device (pick-up coils sensing a 1 Mc signal on the wire) was designed by L. W. Alvarez.

6. These use simple lens formulae. See Jonathan D. Young, Optical Analog for a Symmetric Quadrupole, UCRL-9054, January 1960.

7. These magnets were capable of analyzing momenta as high as 2.35 BeV/c, at which momentum some pion running was done.